Supporting Information

for

Ring-opening homo- and co-polymerization of chiral seven-membered lactones mediated by achiral yttrium catalysts: Insights into the catalyst stereocontrol by mass spectrometry

Ali Dhaini,[a] Jérôme Ollivier,[a] Nicolas Le Yondre,[b] Ali Alaaeddine,[c] Sophie M. Guillaume (ORCID: 0000-0003-2917-8657),[a,*] and Jean-François Carpentier (ORCID: 0000-0002-9160-7662)[a,*]

[a] Univ. Rennes, CNRS, Institut des Sciences Chimiques de Rennes, UMR 6226, F-35042 Rennes, France.

[b] Univ. Rennes, Centre Régional de Mesures Physiques de l'Ouest, UAR 2025 ScanMAT, F-35042 Rennes, France.

[c] Univ. Libanaise, Campus Universitaire Rafic Hariri Hadath, Faculté des Sciences, Laboratoire de Chimie Médicinale et des Produits Naturels, Beirut, Lebanon.

* Corresponding authors: E-mail: sophie.guillaume@univ-rennes.fr, jean francois.carpentier@univ-rennes.fr

Table of contents:

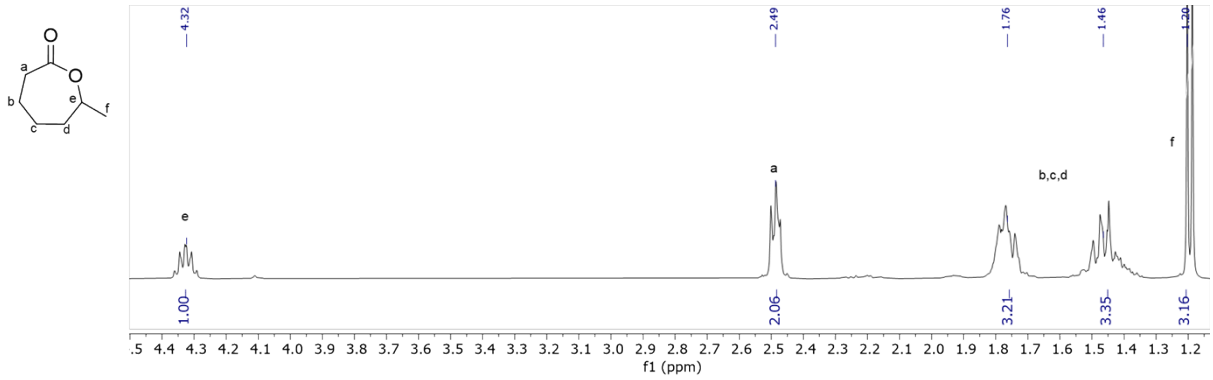

Figure S1. ^{1}H NMR spectrum (400 MHz, $CDCl_3$, 25 °C) of *rac*-CL^{Me}.

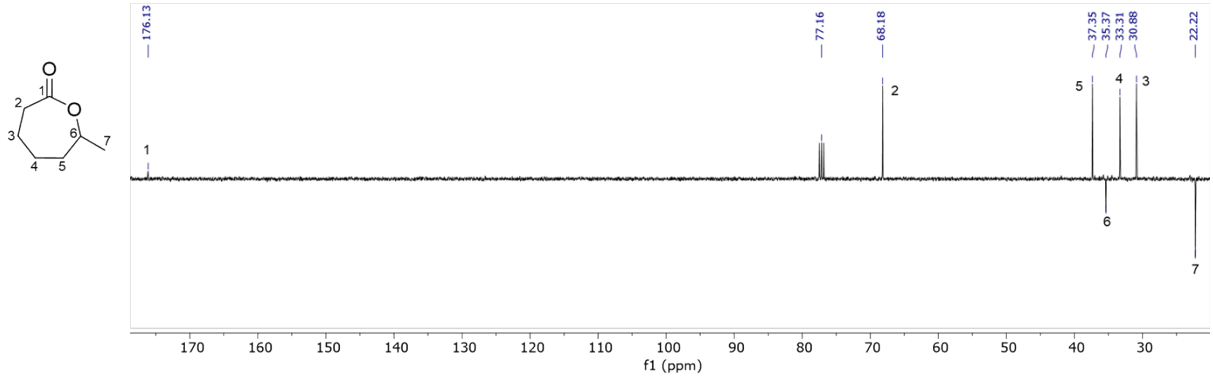

Figure S2. JMOD $^{13}C\{^{1}H\}$ NMR spectrum (125 MHz, $CDCl_3$, 25 °C) of *rac*-CL^{Me}.

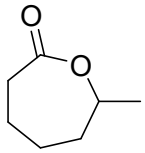

rac-CL^{Me}

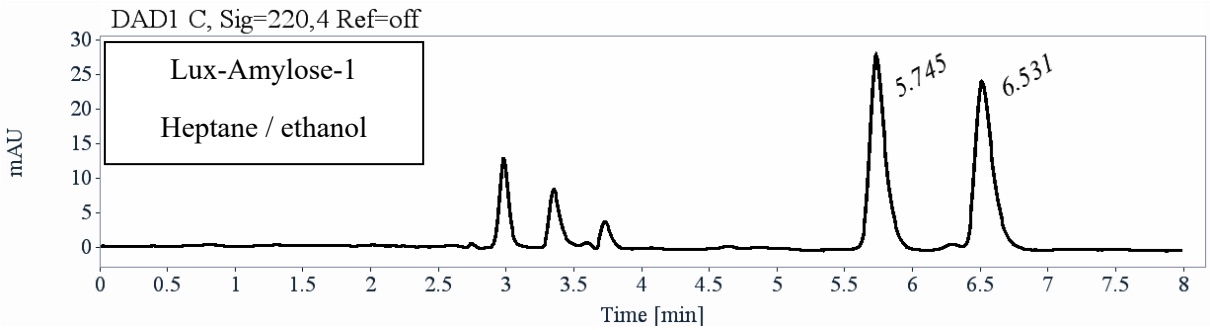

RT [min]	Area	Area%
5.75	232	49.97
6.53	232	50.03
Sum	464	100.00

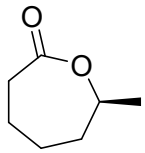

(*S*)-CL^{Me}

• First fraction: the first eluted enantiomer with ee > 99 %

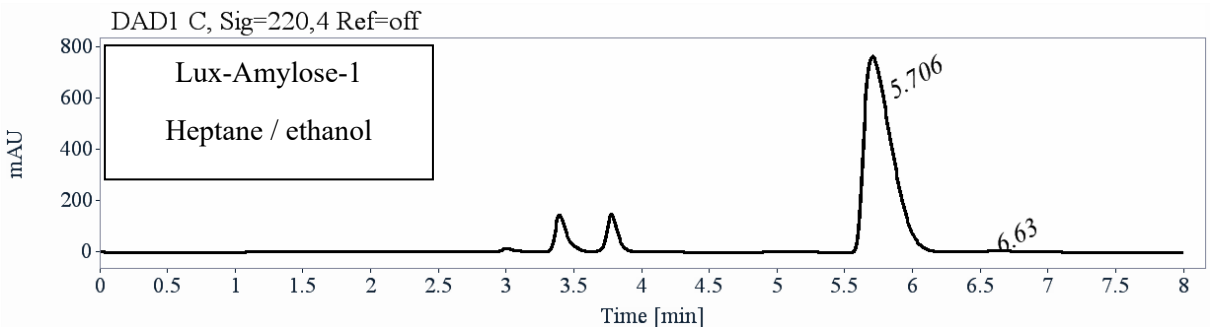

RT [min]	Area	Area%
5.71	10723	99.65
6.63	38	0.35
Sum	10761	100.00

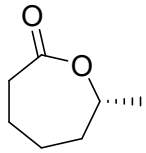

(*R*)-CL^{Me}

• Second fraction: The second eluted enantiomer with ee > 99 %

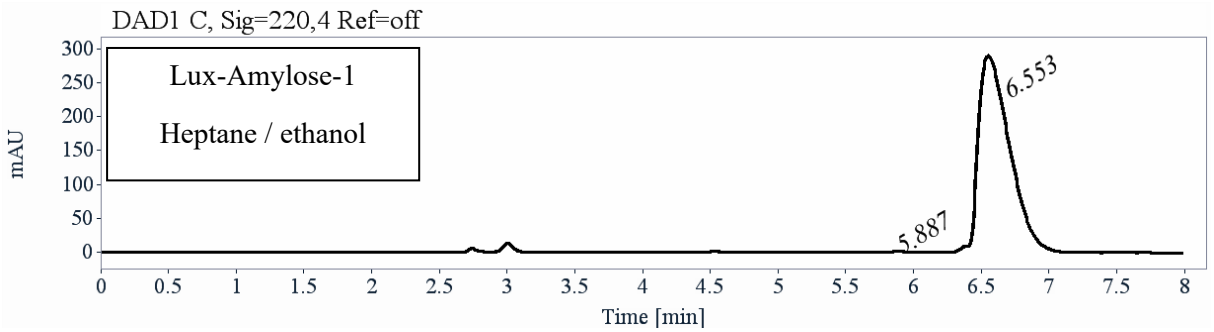

RT [min]	Area	Area%
5.89	16	0.35
6.55	4622	99.65
Sum	4638	100.00

Figure S3. Chiral HPLC traces for *racemic*-CL^{Me}, (*S*)-CL^{Me} and (*R*)-CL^{Me} (see the Experimental section for details)

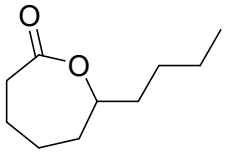

rac - DL

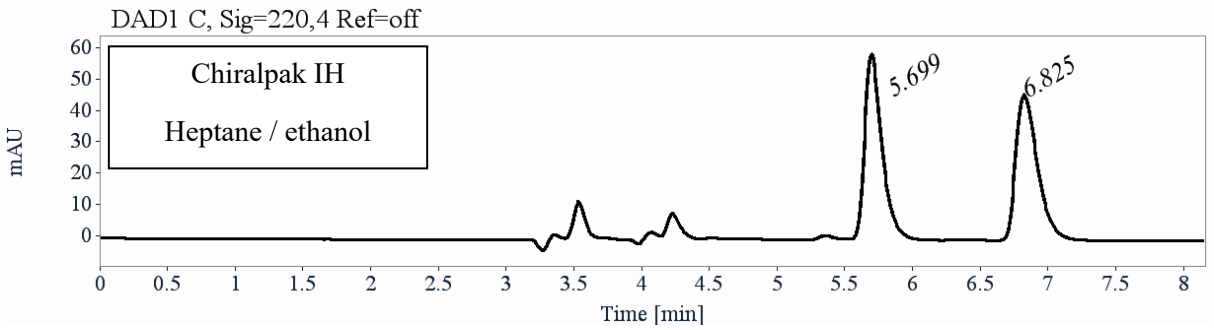

RT [min]	Area	Area%
5.70	521	50.12
6.83	518	49.88
Sum	1039	100.00

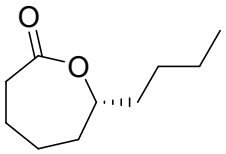

(*R*)-CL$^{n\text{Bu}}$

• First fraction: The first eluted enantiomer with ee > 99.5%

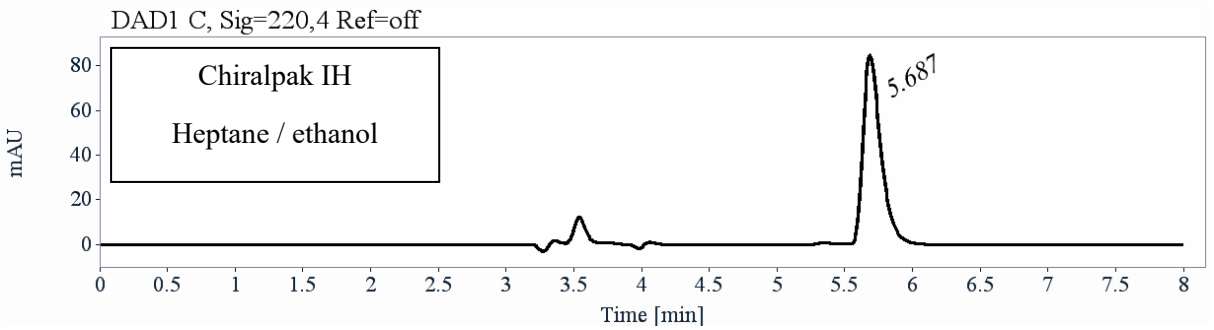

RT [min]	Area	Area%
5.69	767	100.00
Sum	767	100.00

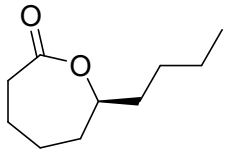

(*S*)-CL$^{n\text{Bu}}$

• Second fraction: The second eluted enantiomer with ee > 99.5 %

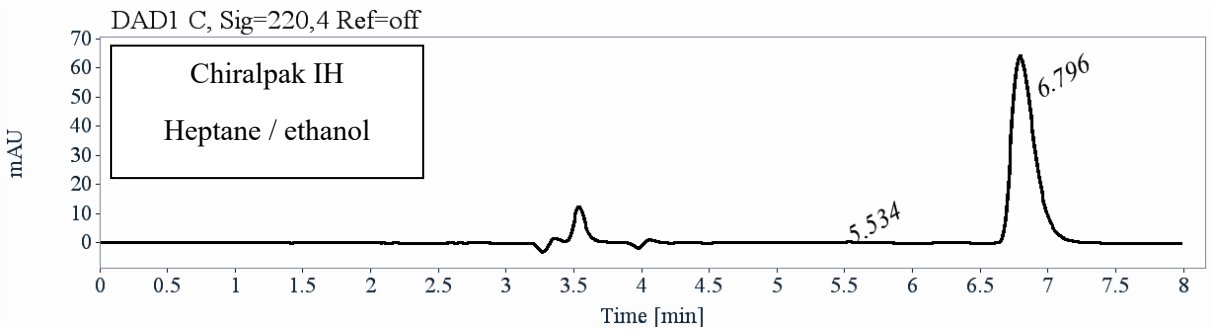

RT [min]	Area	Area%
5.53	2	0.21
6.80	760	99.79
Sum	762	100.00

Figure S4. Chiral HPLC traces for *racemic*-CL$^{n\text{Bu}}$, (*R*)-CL$^{n\text{Bu}}$ and (*S*)-CL$^{n\text{Bu}}$ (see the Experimental section for details)

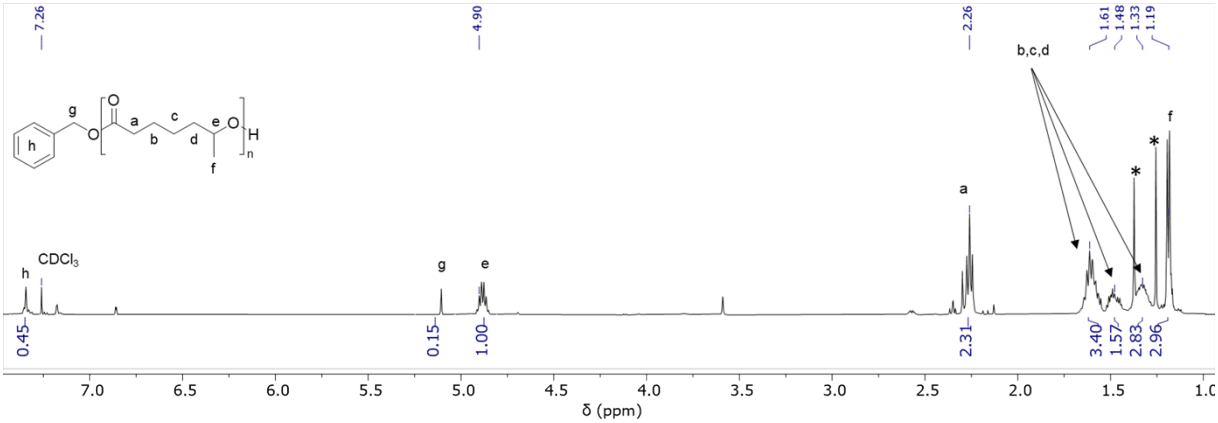

Figure S5. ^{1}H NMR spectrum (500 MHz, $CDCl_3$, 25 °C) of a PCL^{Me} homopolymer prepared from the ROP of *rac*-CL^{Me} (30 equiv) mediated by the **1a**/BnOH (1:1) catalyst system (Table S1, entry 1-105). * stands for resonances of residual solvent and/or catalyst.

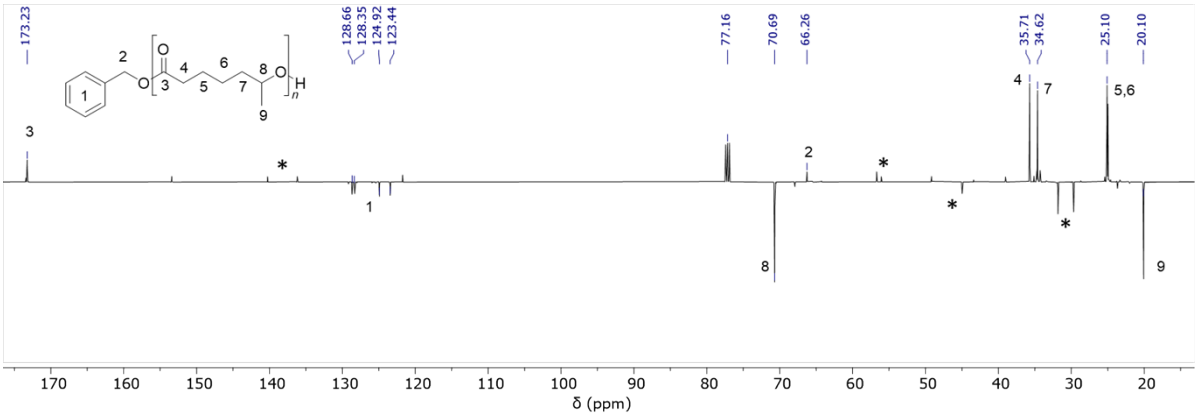

Figure S6. JMOD $^{13}C\{^{1}H\}$ NMR spectrum (125 MHz, $CDCl_3$, 25 °C) of a PCL^{Me} homopolymer prepared from the ROP of *rac*-CL^{Me} (30 equiv) by the **1a**/BnOH (1:1) catalyst system (Table S1, entry 1-105). * stands for resonances of residual solvent and/or catalyst.

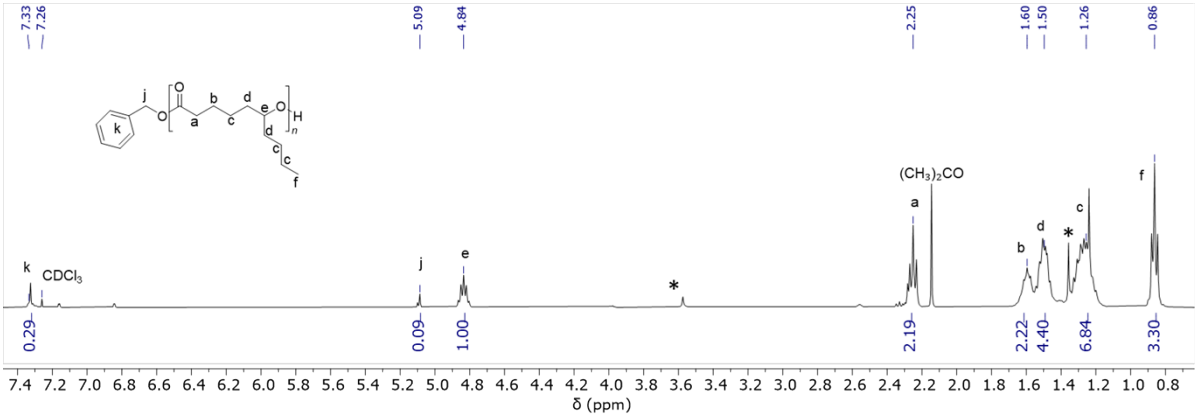

Figure S7. ^{1}H NMR spectrum (500 MHz, $CDCl_3$, 25 °C) of a PCL$^{n\text{Bu}}$ homopolymer prepared from the ROP of *rac*-CL$^{n\text{Bu}}$ (30 equiv) mediated by the **1a**/BnOH (1:1) catalyst system (Table S1, entry 1-107). * stands for resonances of residual solvent and/or catalyst.

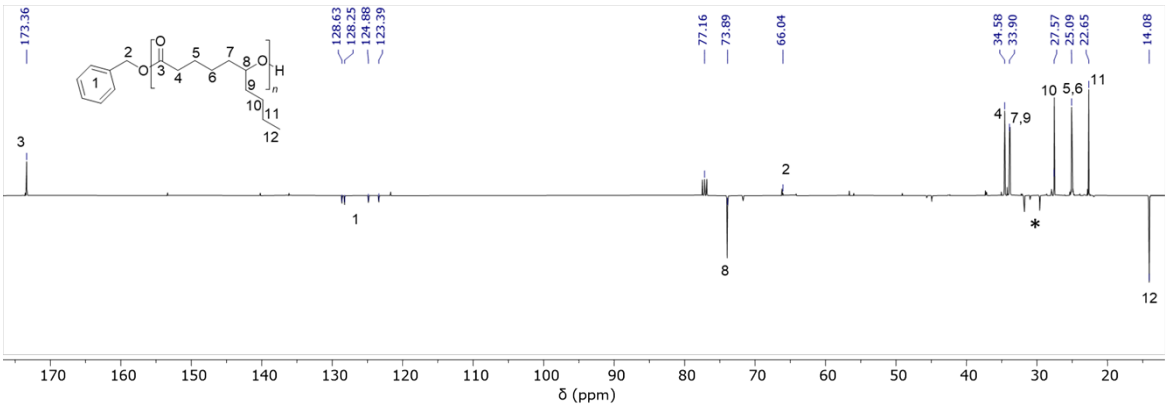

Figure S8. JMOD ^{13}C{^{1}H} spectrum (500 MHz, $CDCl_3$, 25 °C) of a PCL$^{n\text{Bu}}$ homopolymer prepared from the ROP of *rac*-CL$^{n\text{Bu}}$ (30 equiv) mediated by the **1a**/BnOH (1:1) catalyst system (Table S1, entry 1-107). * stands for resonances of residual solvent and/or catalyst.

Table S1. ROP of *rac*-CL^{Me} and *rac*-CL^{nBu} mediated by the **1a**/BnOH, {BDI^{DIPP}}$Zn(NTMS_2)$/BnOH and KO*t*Bu catalyst systems.[a]

	Entry	$[CL^R]_0$ [b] (eq vs. Y)	Catalyst	Time (min)	Conv. $[CL^R]_0$ (%)[c]	$M_{n,theo}$ [d] ($g.mol^{-1}$)	$M_{n,NMR}$ [e] ($g.mol^{-1}$)	$M_{n,SEC}$ [f] ($g.mol^{-1}$)	$Đ_M$ [f]	T_g [g] (°C)
R = Me	1 /1-105	30	**1a**/BnOH	180	100	4000	1500	2700	1.38	–45.9
	2 / 1-117	30	Zn(BDI)/BnOH	120	100	4000	1800	2650	1.20	–52.6
	3 /1-163	60	KO*t*Bu	240	100	7800	nd[i]	nd[h]	nd[h]	nd[h]
	4 / 1-193	60*	Zn(BDI)/BnOH	240	100	7800	4300	nd[h]	nd[h]	–47.7
R = *n*Bu	5 / 1-107	30	**1a**/BnOH	180	100	5200	3700	4700	1.15	–55.4
	6 / 1-114	30	Zn(BDI)/BnOH	120	100	5200	5500	5350	1.17	–55.4
	7 /1-155	60	KO*t*Bu	300	100	10300	[i]	nd[h]	nd[h]	–54.8
	8 /1-164	60*	Zn(BDI)/BnOH	90	100	10300	7600	nd[h]	nd[h]	–56.0

[a] Reactions performed with $[CL^{Me}]_0$ = 1.0 M or $[CL^{nBu}]_0$ = 1.0 M in toluene with [**1a**]/$[BnOH]_0$ = 1:1. [b] Monomer loading. [c] Conversion of CL^{Me} as determined by ^1H NMR analysis of the crude reaction mixture. [d] Calculated according to $M_{n,theo} = [CL^{Me}]_0/[\mathbf{1a}] \times conv.(CL^{Me}) \times M(CL^{Me}) + M(BnOH)$, with $M(CL^{Me})$ = 128 $g.mol^{-1}$ and $M(BnOH)$ = 108 $g.mol^{-1}$. [e] Determined by ^1H NMR analysis of the isolated polymer, from the resonances of the terminal OBn group (refer to Experimental section). [f] Number-average molar mass (uncorrected) and dispersity (M_w/M_n) determined by SEC analysis in THF at 30 °C vs. polystyrene standards; [g] Glass transition temperature as determined by DSC analysis. [h] Not determined. [i] No chain-ends observed due to formation of cyclic polymer. * starting from an enantiopure monomer.

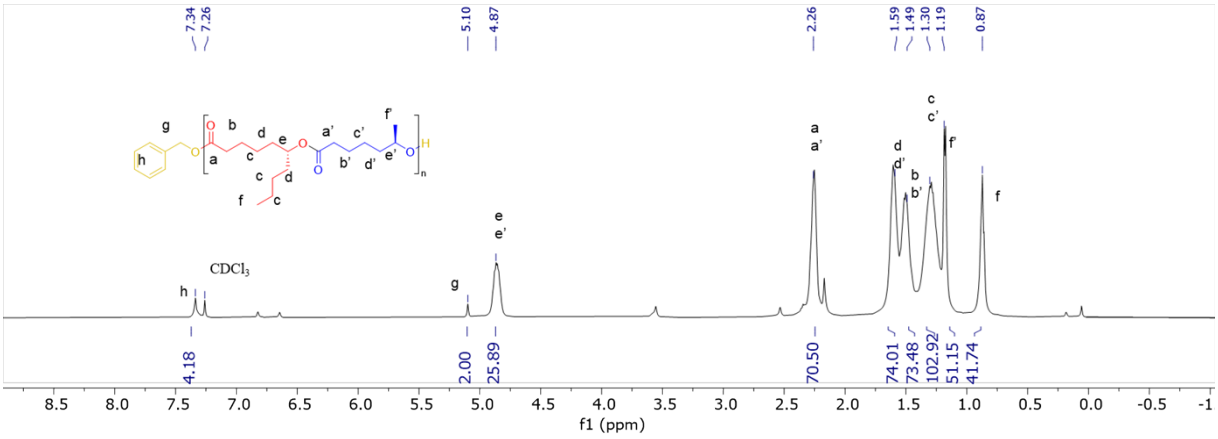

Figure S9. ^{1}H NMR spectrum (400 MHz, $CDCl_3$, 25 °C) of a P(CL^{Me}-*co*-CL^{nBu}) copolymer prepared from the ROCOP of a 1:1 mixture of (*S*)-CL^{Me} and (*R*)-CL^{nBu} mediated by the **1b**/BnOH (1:1) catalyst system (Table 1, entry 6). * stands for resonances of residual solvent and/or catalyst.

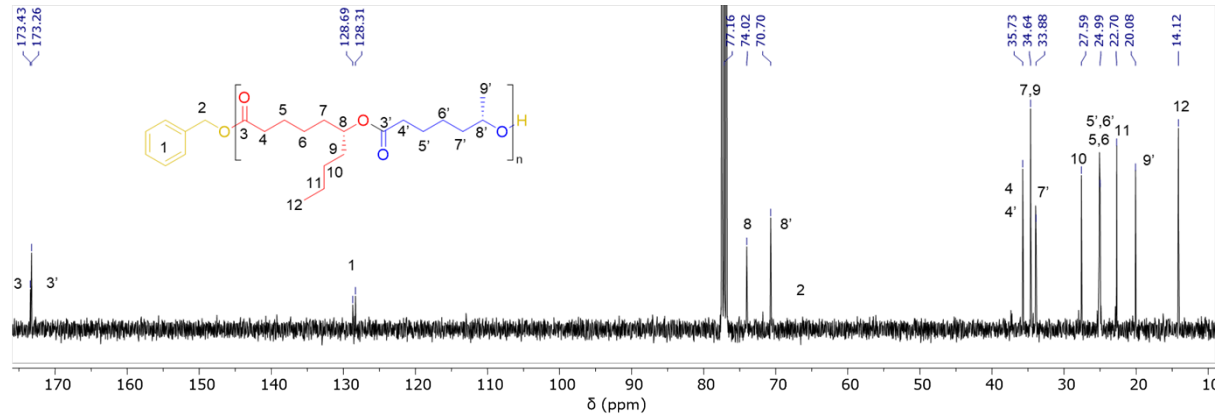

Figure S10. $^{13}C\{^{1}H\}$ NMR spectrum (125 MHz, $CDCl_3$, 25 °C) of a P(CL^{Me}-*co*-CL^{nBu}) copolymer prepared from the ROCOP of a 1:1 mixture of (*S*)-CL^{Me} and (*R*)-CL^{nBu} (1:1) mediated by the **1b**/BnOH (1:1) catalyst system (Table 1, entry 6). * stands for resonances of residual solvent and/or catalyst.

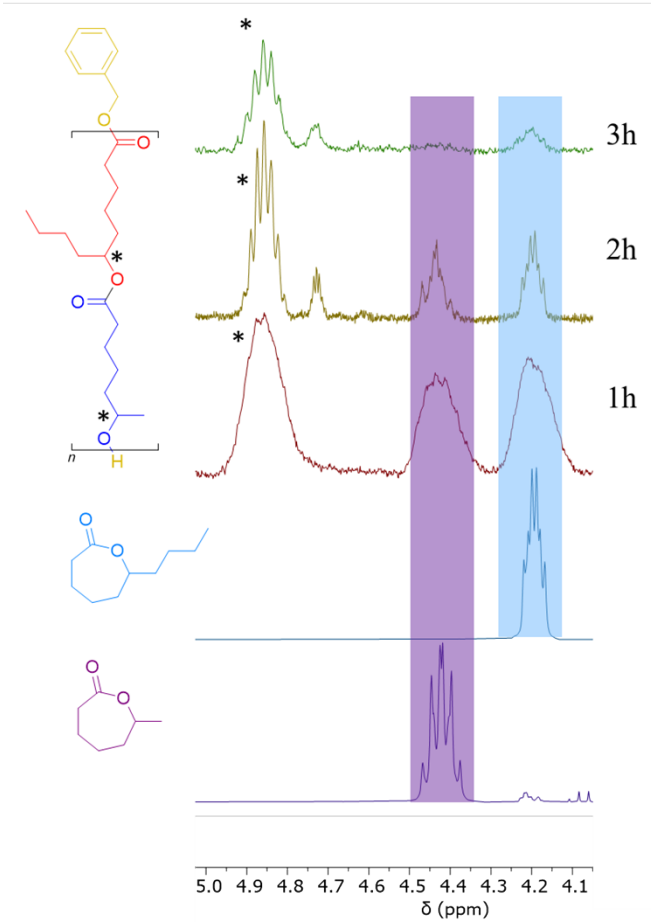

Figure S11. From bottom to top: ^{1}H NMR (400 MHz, $CDCl_3$, 25 °C) spectra of the starting comonomers; ^{1}H NMR (400 MHz, $CDCl_3$, 25 °C) spectra for the monitoring of the ROCOP of a 1:1 mixture of (*R*)-CL^{nBu} and (*S*)-CL^{Me} mediated by the **1b**/BnOH (1:1) catalyst system at 20 °C. Reaction time = 1 h: conv(CL^{nBu} / CL^{Me}) = 58 and 62% respectively; ratio (CL^{nBu} / CL^{Me}) = 1.14. Reaction time = 2 h: conv(CL^{nBu} / CL^{Me}) = 71 and 72%, respectively; ratio (CL^{nBu} / CL^{Me}) = 1.05. Reaction time = 4 h: conv(CL^{nBu} / CL^{Me}) = 90 and 99%, respectively; ratio (CL^{nBu} / CL^{Me}) = 10. * stands for resonances of the copolymer.

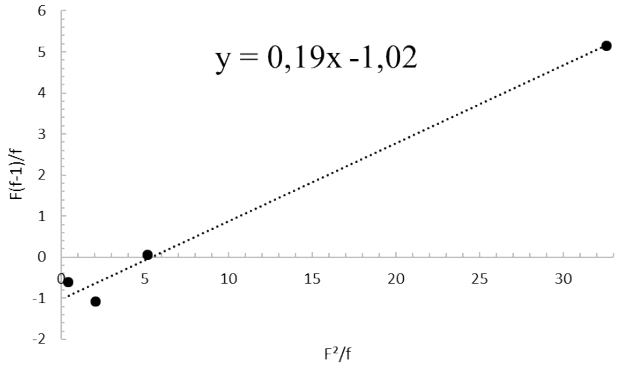

Figure S12. Fineman –Ross plot for the determination of monomer reactivity ratio of CL^{Me} and CL^{nBu} in the copolymerization by the **1a**/BnOH (1:1) system in toluene at 20 °C.

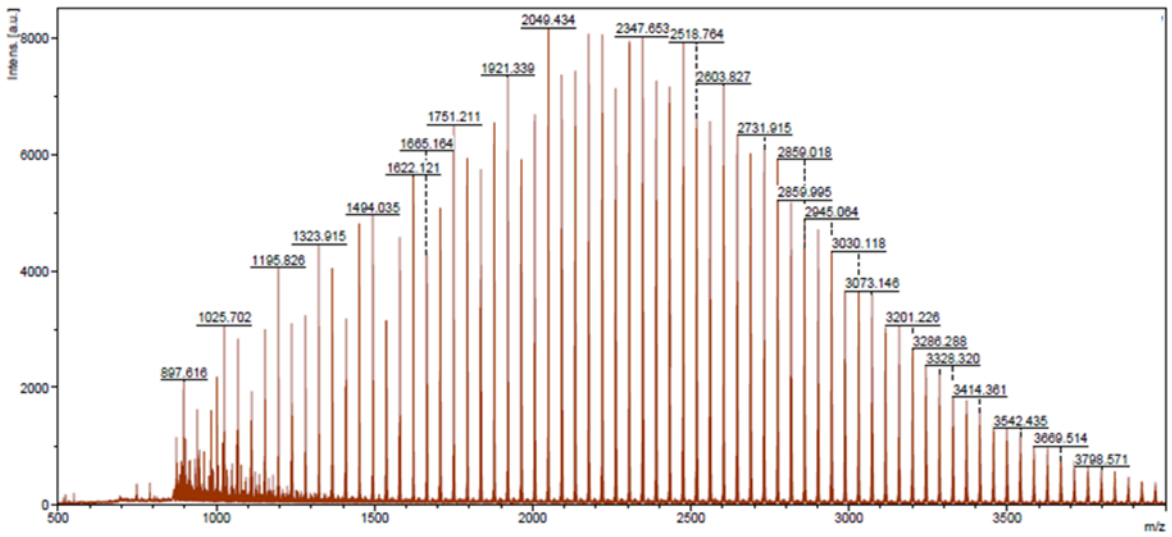

Figure S13. MALDI-ToF mass spectrum (DCTB matrix, ionized by Na^+) of a P(CL^{Me}-*co*-CL^{nBu}) copolymer prepared by ROCOP of (*S*)-CL^{Me} and (*R*)-CL^{nBu} (1:1) with the **1b**/BnOH catalyst system (Table 1, entry 6).

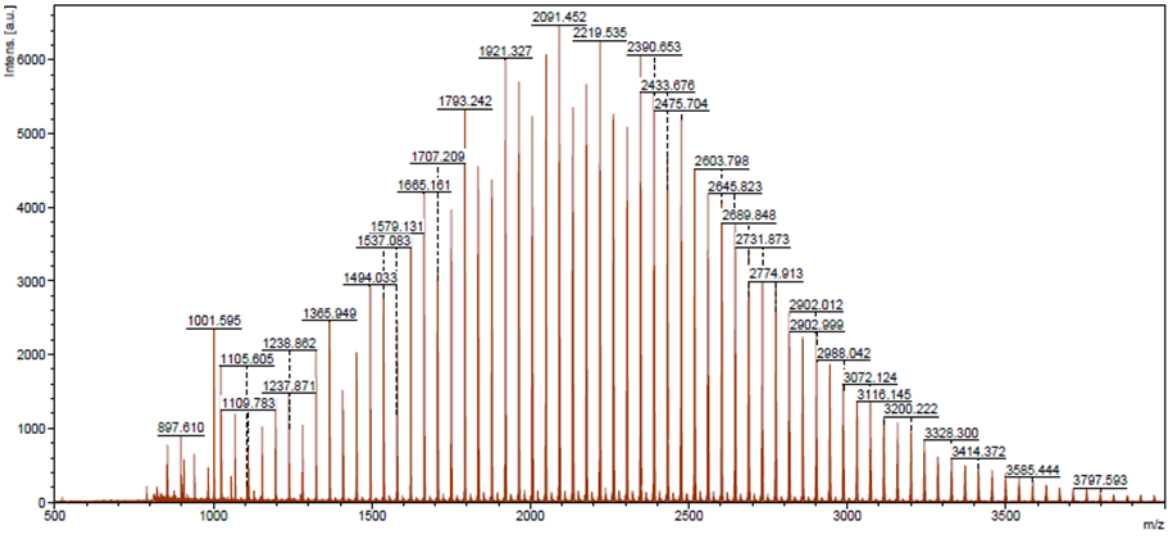

Figure S14. MALDI-ToF mass spectrum (DCTB matrix, ionized by Na^+) of a P(CL^{Me}-*co*-CL^{nBu}) copolymer prepared by ROCOP of (*S*)-CL^{Me} and (*R*)-CL^{nBu} (1:1) with the **1a**/BnOH catalyst system (Table 1, entry 2).

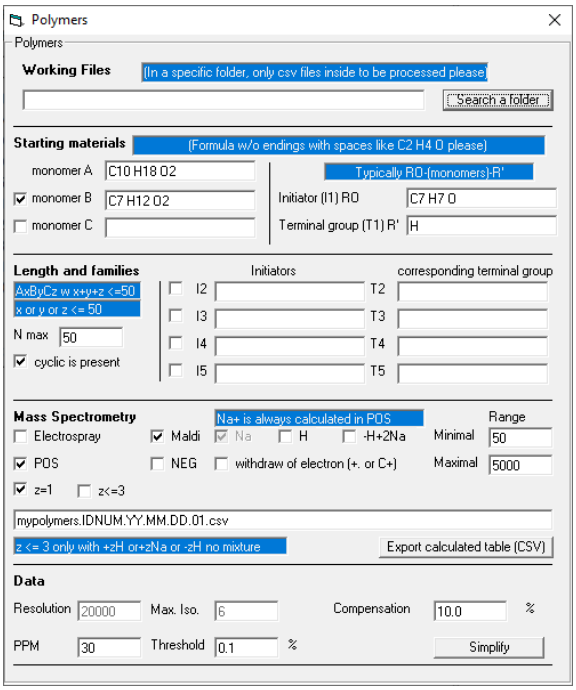

Figure S15. "Polymers" software for automatic generation of theoretical *m/z* peaks and assignment to experimental *m/z* mass peaks.

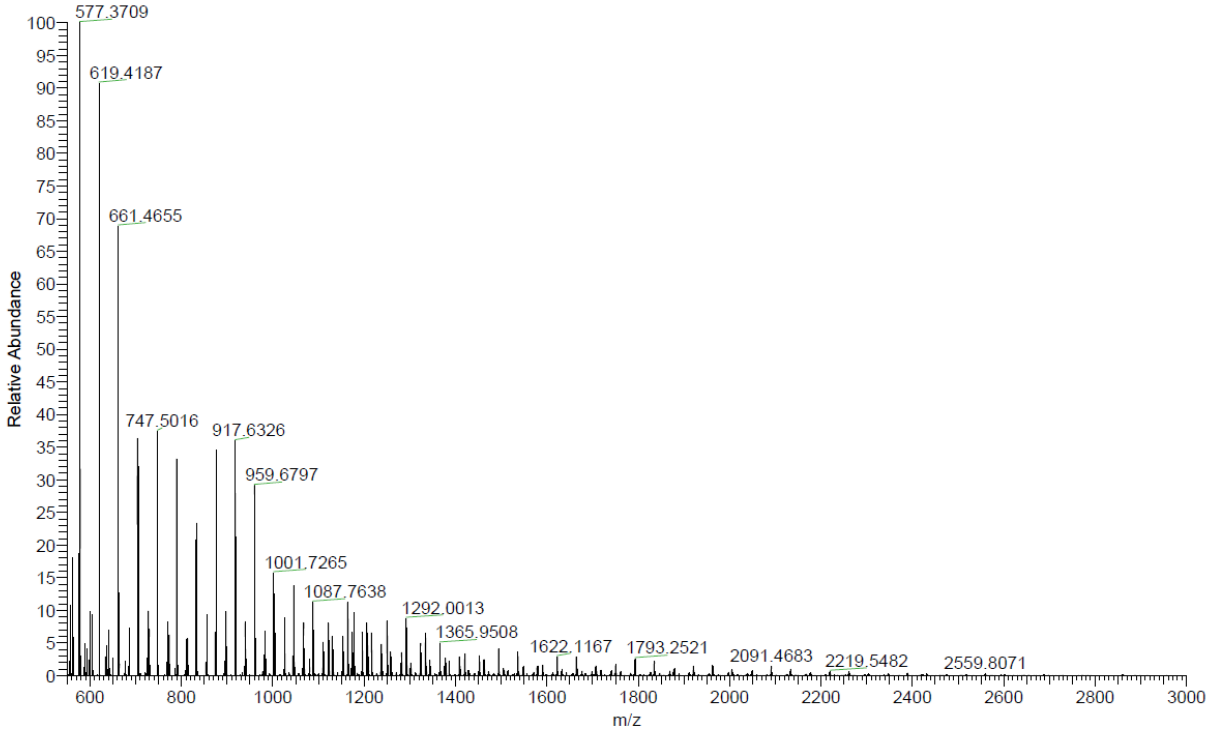

Figure S16. ESI-mass spectrum (solvent CH_2Cl_2) of a P(CL^{Me}-*co*-CL^{nBu}) copolymer prepared by ROCOP of a 1:1 mixture of (*S*)-CL^{Me} and (*R*)-CL^{nBu} with the **1a**/BnOH catalyst system (Table 1, entry 3).

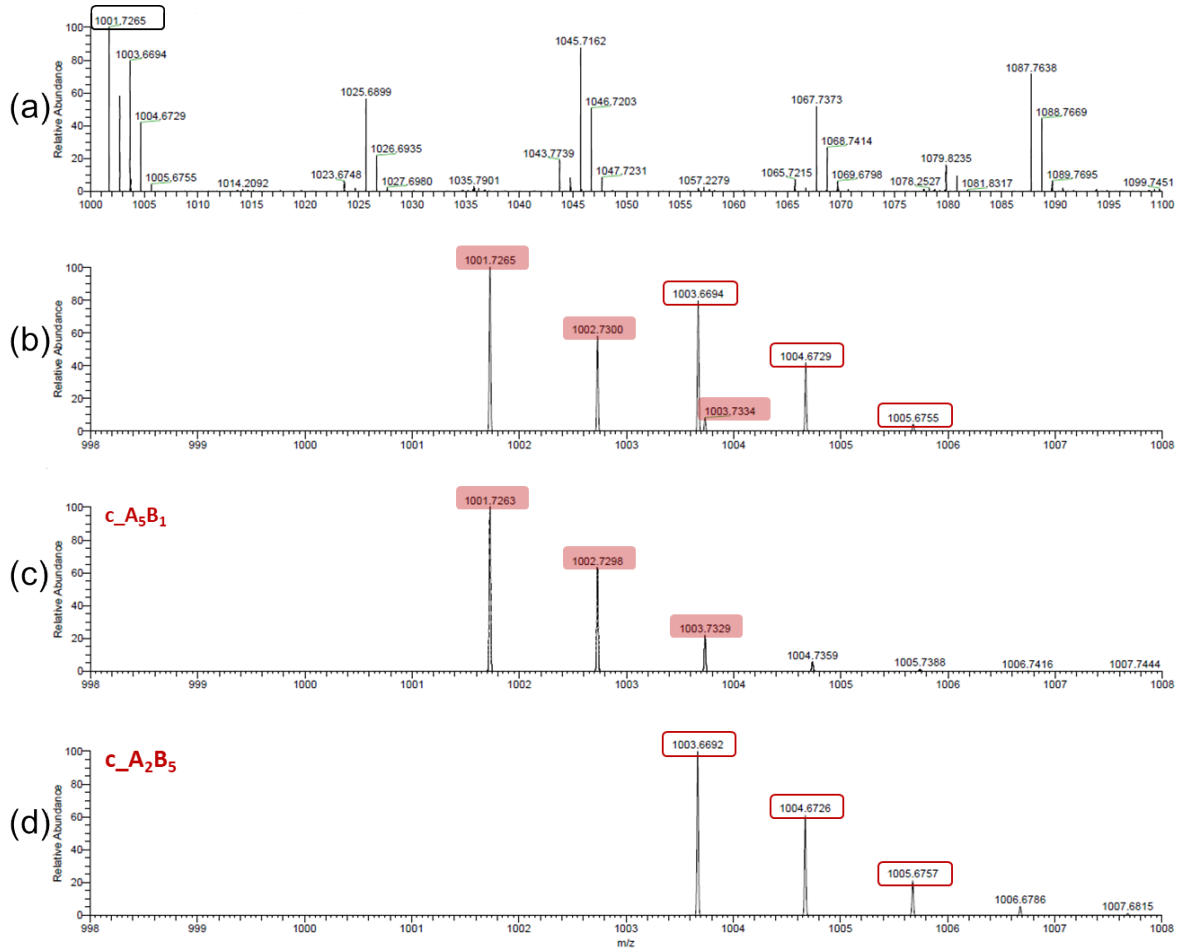

Figure S17. Details of the high resolution ESI mass spectra of a P(CL$^{n\text{Bu}}$-*co*-CL$^{\text{Me}}$) copolymer prepared by ROCOP of a 1:1 mixture of (*R*)-CL$^{n\text{Bu}}$ and (*S*)-CL$^{\text{Me}}$ with the **1a**/BnOH catalyst system (Table 1, entry 3), from top to bottom: (a) experimental spectrum (solvent: CH_2Cl_2) for *m/z* = 1000–1100, (b) zoomed region for *m/z* = 998–1008, showing resolved peaks for cyclic P[(CL$^{n\text{Bu}}$)$_5$-*co*-(CL$^{\text{Me}}$)] (m/z_{exp} (all ^{12}C) = 1001.7265) and cyclic P[(CL$^{n\text{Bu}}$)$_2$-*co*-(CL$^{\text{Me}}$)$_5$] (m/z_{exp} (all ^{12}C) = 1003.6694); (c) calculated spectrum (isotopic pattern) for cyclic P[(CL$^{n\text{Bu}}$)$_5$-*co*-(CL$^{\text{Me}}$)] (m/z_{calcd} (all ^{12}C) = 1001.7263); (d) calculated spectrum (isotopic pattern) for cyclic P[(CL$^{n\text{Bu}}$)$_2$-*co*-(CL$^{\text{Me}}$)$_5$] (m/z_{calcd} (all ^{12}C) = 1003.6692).

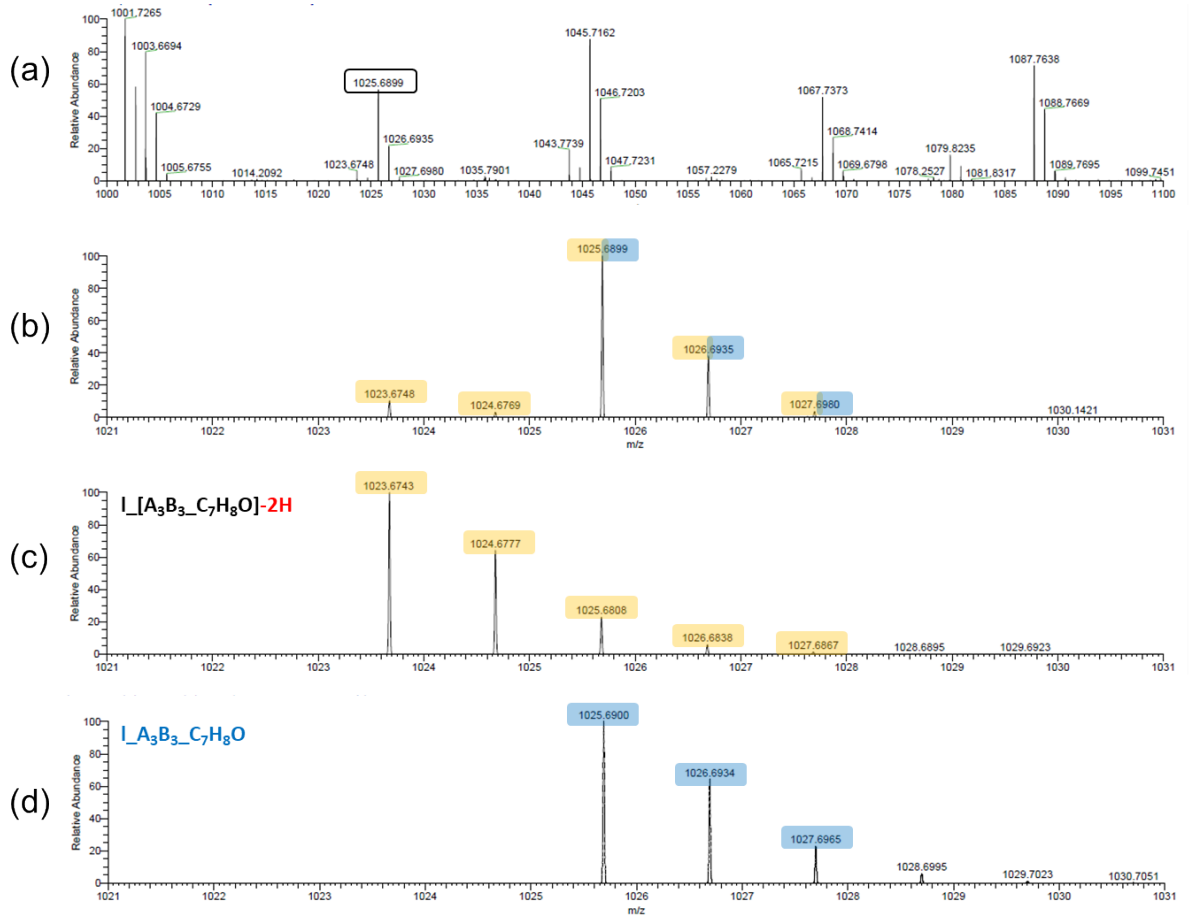

Figure S18. Details of the high resolution ESI mass spectra of a P(CL$^{n\text{Bu}}$-*co*-CL$^{\text{Me}}$) copolymer prepared by ROCOP of a 1:1 mixture of (*R*)-CL$^{n\text{Bu}}$ and (*S*)-CL$^{\text{Me}}$ with the **1a**/BnOH catalyst system (Table 1, entry 3), from top to bottom: (a) experimental spectrum (solvent: CH_2Cl_2) for *m/z* = 1000–1100, (b) zoomed region for *m/z* = 1021-1031, showing resolved peaks for linear P[(CL$^{n\text{Bu}}$)$_3$-*co*-(CL$^{\text{Me}}$)$_3$]-C_7H_8O – 2H (m/z_{exp} (all ^{12}C) = 1023.6748) and linear P[(CL$^{n\text{Bu}}$)$_3$-*co*-(CL$^{\text{Me}}$)$_3$]-C_7H_8O (m/z_{exp} (all ^{12}C) = 1025.6899); (c) calculated spectrum (isotopic pattern) for cyclic linear P[(CL$^{n\text{Bu}}$)$_3$-*co*-(CL$^{\text{Me}}$)$_3$]-C_7H_8O – 2H (m/z_{calcd} (all ^{12}C) = 1023.6743); (d) calculated spectrum (isotopic pattern) for linear P[(CL$^{n\text{Bu}}$)$_3$-*co*-(CL$^{\text{Me}}$)$_3$]-C_7H_8O (m/z_{calcd} (all ^{12}C) = 1025.6900).

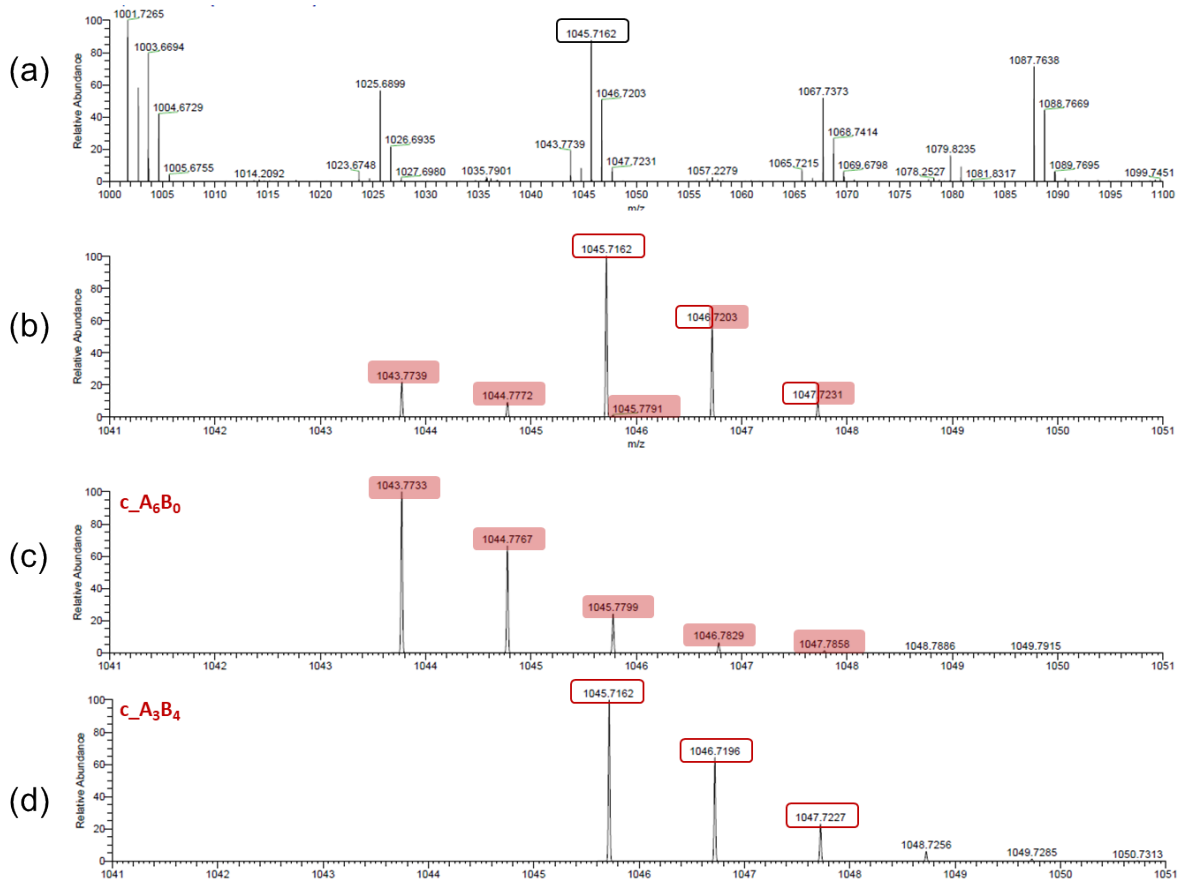

Figure S19. Details of the high resolution ESI mass spectra of a P(CL$^{n\text{Bu}}$-*co*-CL$^{\text{Me}}$) copolymer prepared by ROCOP of a 1:1 mixture of (*R*)-CL$^{n\text{Bu}}$ and (*S*)-CL$^{\text{Me}}$ with the **1a**/BnOH catalyst system (Table 1, entry 3), from top to bottom: (a) experimental spectrum (solvent: CH_2Cl_2) for *m/z* = 1000–1100, (b) zoomed region for *m/z* = 1041-1051, showing resolved peaks for cyclic P[(CL$^{n\text{Bu}}$)$_6$-*co*-(CL$^{\text{Me}}$)$_0$] (m/z_{exp} (all ^{12}C) = 1043.7739) and cyclic P[(CL$^{n\text{Bu}}$)$_3$-*co*-(CL$^{\text{Me}}$)$_4$] (m/z_{exp} (all ^{12}C) = 1045.7162); (c) calculated spectrum (isotopic pattern) for cyclic P[(CL$^{n\text{Bu}}$)$_6$-*co*-(CL$^{\text{Me}}$)$_0$] (m/z_{calcd} (all ^{12}C) = 1043.7733); (d) calculated spectrum (isotopic pattern) for cyclic P[(CL$^{n\text{Bu}}$)$_3$-*co*-(CL$^{\text{Me}}$)$_4$] (m/z_{calcd} (all ^{12}C) = 1045.7162).

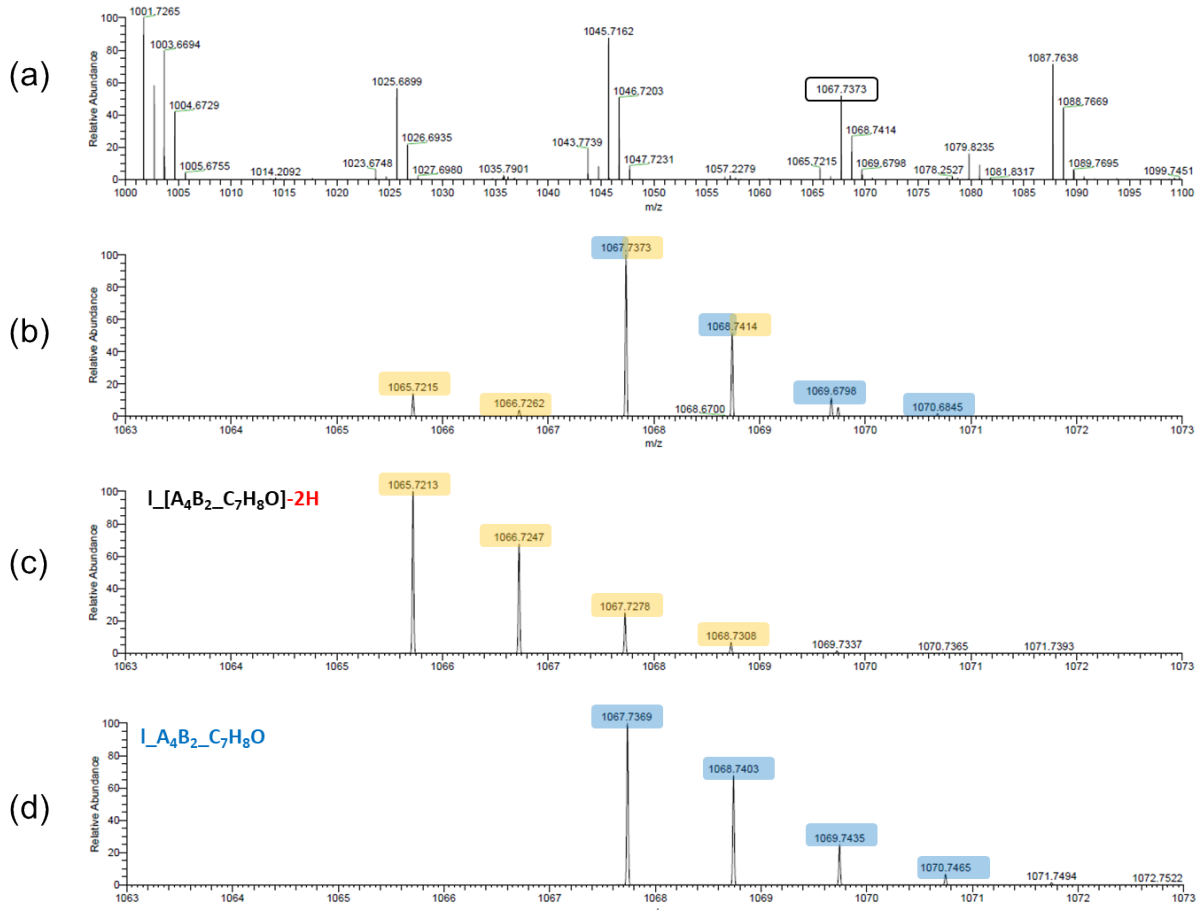

Figure S20. Details of the high resolution ESI mass spectra of a P(CL$^{n\text{Bu}}$-*co*-CL$^{\text{Me}}$) copolymer prepared by ROCOP of a 1:1 mixture of (*R*)-CL$^{n\text{Bu}}$ and (*S*)-CL$^{\text{Me}}$ with the **1a**/BnOH catalyst system (Table 1, entry 3), from top to bottom: (a) experimental spectrum (solvent: CH_2Cl_2) for *m/z* = 1000–1100, (b) zoomed region for *m/z* = 1063-1073, showing resolved peaks for linear P[(CL$^{n\text{Bu}}$)$_4$-*co*-(CL$^{\text{Me}}$)$_2$]-C_7H_8O – 2H (*m/z*$_{\text{exp}}$ (all ^{12}C) = 1065.7215) and linear P[(CL$^{n\text{Bu}}$)$_4$-*co*-(CL$^{\text{Me}}$)$_2$]-C_7H_8O (*m/z*$_{\text{exp}}$ (all ^{12}C) = 1067.7373); (c) calculated spectrum (isotopic pattern) for cyclic linear P[(CL$^{n\text{Bu}}$)$_4$-*co*-(CL$^{\text{Me}}$)$_2$]-C_7H_8O – 2H (*m/z*$_{\text{calcd}}$ (all ^{12}C) = 1065.7213); (d) calculated spectrum (isotopic pattern) for linear P[(CL$^{n\text{Bu}}$)$_4$-*co*-(CL$^{\text{Me}}$)$_2$]-C_7H_8O (*m/z*$_{\text{calcd}}$ (all ^{12}C) = 1067.7369).

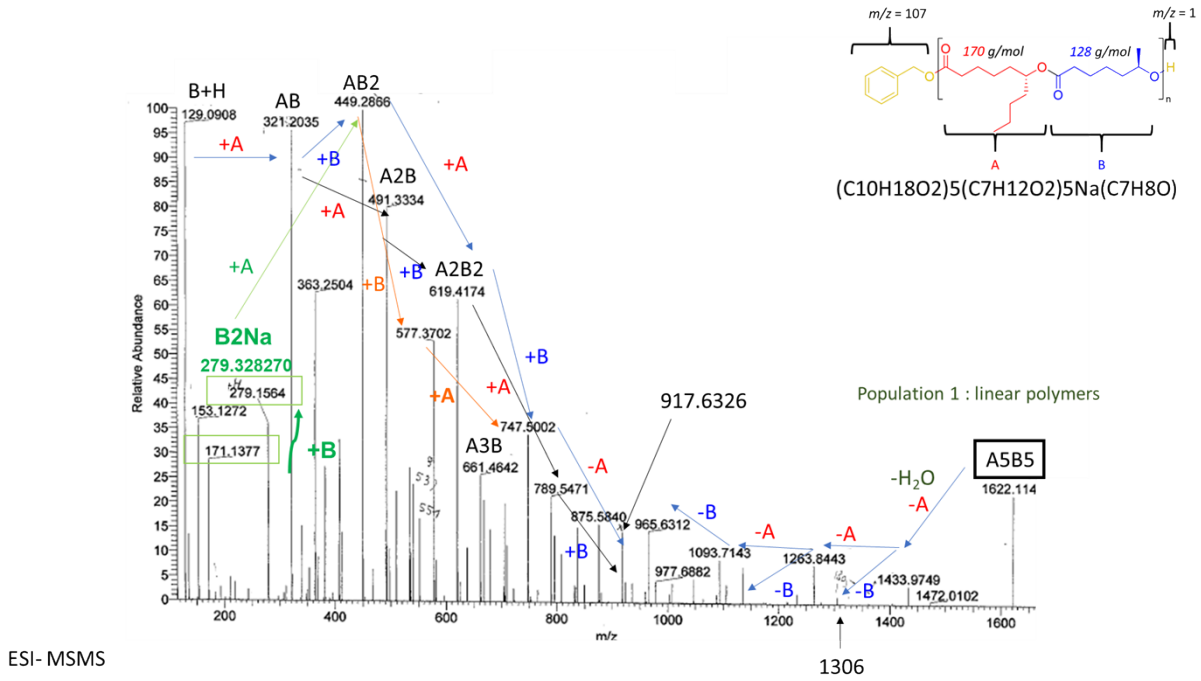

Figure S21. MS/MS fragmentation ESI mass spectrum of the ion *m/z* = 1622 of a P(CL^{Me}-*co*-CL^{nBu}) **copolymer** prepared by ROCOP of a 1:1 mixture of (*S*)-CL^{Me} and (*R*)-CL^{nBu} with the **1a**/BnOH catalyst system (Table 1, entry 3).

Table S2. Comparison of theoretical vs. experimental ESI-MS peaks for a P(CL^{nBu}-*co*-CL^{Me}) copolymer (Table 1, entry 3) for *m/z* values in the range 200–1800. A: stands for CL^{nBu} and *x* for the number of A units in the polymer chain, B: stands for CL^{Me} and *y* for the number of B units in the polymer chain. All non-assigned peaks or beyond the range are excluded from that table.

m/z theoritical	Interpretation AxBy	Raw Formula	Population	x	y	x+y	m/z experimental HR-ESI	Erreur (PPM) HR-ESI	Absolute Intensity ESI	m/z experimental MALDI-TOF	Erreur (PPM) MALDI	Absolute Intensity MALDI-TOF
619,4180	c_A2B2	C34H60O8Na	Cyclic	2	2	4	619,4187	1,06	6306631,5	619,4209122	4,635268226	2638
641,4388	l_A3B0_C7H8O	C37H62O7Na	C7H7O_H	3	0	3	641,4397	1,45	485720,6	641,4464819	12,02131196	2099
661,4650	c_A3B1	C37H66O8Na	Cyclic	3	1	4	661,4655	0,77	4867532,5	661,4697684	7,222499419	3666
685,4286	l_A1B3_C7H8O	C38H62O9Na	C7H7O_H	1	3	4	685,4289	0,44	496851,2	685,4387311	14,77928334	750
703,5119	c_A4B0	C40H72O8Na	Cyclic	4	0	4	703,5117	0,34	2556988,5	703,5125391	0,850132706	3069
705,4548	c_A1B4	C38H66O10Na	Cyclic	1	4	5	705,4545	0,46	2196333,3	705,4585526	5,289620201	628
727,4756	l_A2B2_C7H8O	C41H68O9Na	C7H7O_H	2	2	4	727,4761	0,75	693295,1	727,4750194	0,730751202	1155
747,5018	c_A2B3	C41H72O10Na	Cyclic	2	3	5	747,5016	0,23	2573951,3	747,4993582	3,227806141	1478
769,5225	l_A3B1_C7H8O	C44H74O9Na	C7H7O_H	3	1	4	769,5229	0,52	574137	769,5241934	2,199265591	1958
789,5487	c_A3B2	C44H78O10Na	Cyclic	3	2	5	789,5488	0,1	2297048,3	789,5467073	2,550451753	2560
811,5695	l_A4B0_C7H8O	C47H80O9Na	C7H7O_H	4	0	4	811,5696	0,18	395667,6	811,5678006	2,033587107	2064
831,5957	c_A4B1	C47H84O10Na	Cyclic	4	1	5	831,5955	0,21	1460930,4	831,5929689	3,249295153	2489
855,5593	l_A2B3_C7H8O	C48H80O11Na	C7H7O_H	2	3	5	855,5594	0,14	646397,9	855,5558882	3,96560253	933
873,6426	c_A5B0	C50H90O10Na	Cyclic	5	0	5	873,6428	0,2	453784,1	873,6378063	5,511060365	924
875,5855	c_A2B4	C48H84O12Na	Cyclic	2	4	6	875,5851	0,46	2424710,5	875,5818101	4,215372489	925
897,6062	l_A3B2_C7H8O	C51H86O11Na	C7H7O_H	3	2	5	897,6064	0,19	678449,1	897,6007829	6,069565943	1538
917,6325	c_A3B3	C51H90O12Na	Cyclic	3	3	6	917,6326	0,16	2543615,5	917,6305572	2,063836173	1472
939,6532	l_A4B1_C7H8O	C54H92O11Na	C7H7O_H	4	1	5	939,6535	0,34	579489,4	939,653184	0,003215502	2940
959,6794	c_A4B2	C54H96O12Na	Cyclic	4	2	6	959,6797	0,31	2045526,5	959,6771023	2,395272852	1696
981,7001	l_A5B0_C7H8O	C57H98O11Na	C7H7O_H	5	0	5	981,6997	0,44	217275,3	981,6979628	2,208639384	2016
983,6430	l_A2B4_C7H8O	C55H92O13Na	C7H7O_H	2	4	6	983,6426	0,42	466782,6	983,6403726	2,682298859	713
1001,7264	c_A5B1	C57H102O12Na	Cyclic	5	1	6	1001,7265	0,15	1080027,5	1001,727785	1,431176302	1421
1003,6692	c_A2B5	C55H96O14Na	Cyclic	2	5	7	1003,6694	0,17	862981,1	1003,65947	9,725776245	614
1025,6900	l_A3B3_C7H8O	C58H98O13Na	C7H7O_H	3	3	6	1025,6899	0,06	608170,3	1025,685443	4,404456609	1609
1043,7733	c_A6B0	C60H108O12Na	Cyclic	6	0	6	1043,7739	0,57	208898,2	1043,766152	6,849451662	298
1045,7162	c_A3B4	C58H102O14Na	Cyclic	3	4	7	1045,7162	0,02	949886,9	1045,714404	1,699239105	1098
1067,7369	l_A4B2_C7H8O	C61H104O13Na	C7H7O_H	4	2	6	1067,7373	0,36	558374,5	1067,734004	2,722872025	3041
1087,7631	c_A4B3	C61H108O14Na	Cyclic	4	3	7	1087,7638	0,62	788434,4	1087,75637	6,215139708	1579
1109,7839	l_A5B1_C7H8O	C64H110O13Na	C7H7O_H	5	1	6	1109,784	0,13	351197,5	1109,779651	3,793666763	3651
1129,8101	c_A5B2	C64H114O14Na	Cyclic	5	2	7	1129,8105	0,37	411308,2	1129,802735	6,502269313	1233
1153,7737	l_A3B4_C7H8O	C65H110O15Na	C7H7O_H	3	4	7	1153,7739	0,18	408306,7	1153,768429	4,560716281	1578
1171,8570	c_A6B1	C67H120O14Na	Cyclic	6	1	7	1171,8582	1	76918,2	1171,850544	5,535436594	678
1173,7999	c_A3B5	C65H114O16Na	Cyclic	3	5	8	1173,801	0,93	453022,8	1173,795824	3,481656988	919
1195,8206	l_A4B3_C7H8O	C68H116O15Na	C7H7O_H	4	3	7	1195,8211	0,38	459051,6	1195,813165	6,251802363	3403
1215,8469	c_A4B4	C68H120O16Na	Cyclic	4	4	8	1215,8471	0,2	453720,5	1215,839158	6,335628856	1246
1237,8676	l_A5B2_C7H8O	C71H122O15Na	C7H7O_H	5	2	7	1237,8672	0,32	337771,8	1237,860334	5,862396448	4954
1257,8938	c_A5B3	C71H126O16Na	Cyclic	5	3	8	1257,8944	0,47	253078,7	1257,882093	9,315650105	1442
1279,9145	l_A6B1_C7H8O	C74H128O15Na	C7H7O_H	6	1	7	1279,9147	0,12	130310,8	1279,905874	6,771300552	4127
1281,8574	l_A3B5_C7H8O	C72H122O17Na	C7H7O_H	3	5	8	1281,8567	0,56	244319,7	1281,880635	18,10985424	1905
1299,9408	c_A6B2	C74H132O16Na	Cyclic	6	2	8	1299,94	0,59	75080,4	1299,933508	5,579320547	1132
1301,8836	c_A3B6	C72H126O18Na	Cyclic	3	6	9	1301,8841	0,35	132025	1301,894979	8,708942305	670
1323,9044	l_A4B4_C7H8O	C75H128O17Na	C7H7O_H	4	4	8	1323,9037	0,51	344210,5	1323,891908	9,413562936	3681
1343,9306	c_A4B5	C75H132O18Na	Cyclic	4	5	9	1343,9307	0,08	164776,5	1343,92318	5,514457475	1237
1365,9513	l_A5B3_C7H8O	C78H134O17Na	C7H7O_H	5	3	8	1365,9508	0,38	348090,8	1365,935234	11,77684624	6024
1385,9775	c_A5B4	C78H138O18Na	Cyclic	5	4	9	1385,977	0,39	153601,6	1385,961438	11,61829447	1518
1407,9983	l_A6B2_C7H8O	C81H140O17Na	C7H7O_H	6	2	8	1407,9964	1,33	197370,3	1407,984568	9,731936579	6712
1409,9412	l_A3B6_C7H8O	C79H134O19Na	C7H7O_H	3	6	9	1409,9409	0,18	98665,2	1409,971772	21,71790733	2641
1428,0245	c_A6B3	C81H144O18Na	Cyclic	6	3	9	1428,0234	0,76	53733,2	1428,01104	9,419649708	1161
1450,0452	l_A7B1_C7H8O	C84H146O17Na	C7H7O_H	7	1	8	1450,0472	1,36	42270,5	1450,030103	10,42602319	3382
1451,9881	l_A4B5_C7H8O	C82H140O19Na	C7H7O_H	4	5	9	1451,9868	0,9	216783,5	1451,990387	1,574424404	3552
1494,0351	l_A5B4_C7H8O	C85H146O19Na	C7H7O_H	5	4	9	1494,0331	1,31	286080	1494,014932	13,46639192	6146
1514,0613	c_A5B5	C85H150O20Na	Cyclic	5	5	10	1514,0596	1,1	47504	1514,042471	12,41678008	1049
1536,0820	l_A6B3_C7H8O	C88H152O19Na	C7H7O_H	6	3	9	1536,0811	0,59	246633,4	1536,058751	15,13588187	7607

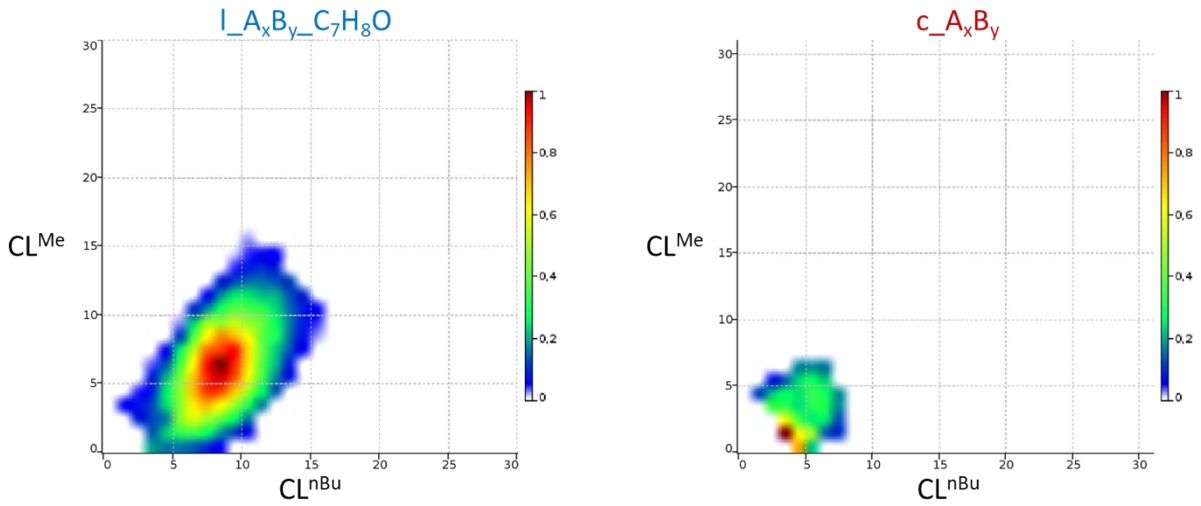

Figure S22. Contour-plots generated by the COCONUT software[i] from MALDI-ToF MS data of a P(CL$^{n\text{Bu}}$)$_x$-*co*-(CL$^{\text{Me}}$)$_y$ copolymer **(Left: linear population; Right: cyclic population) (Table 1, entry 3).**

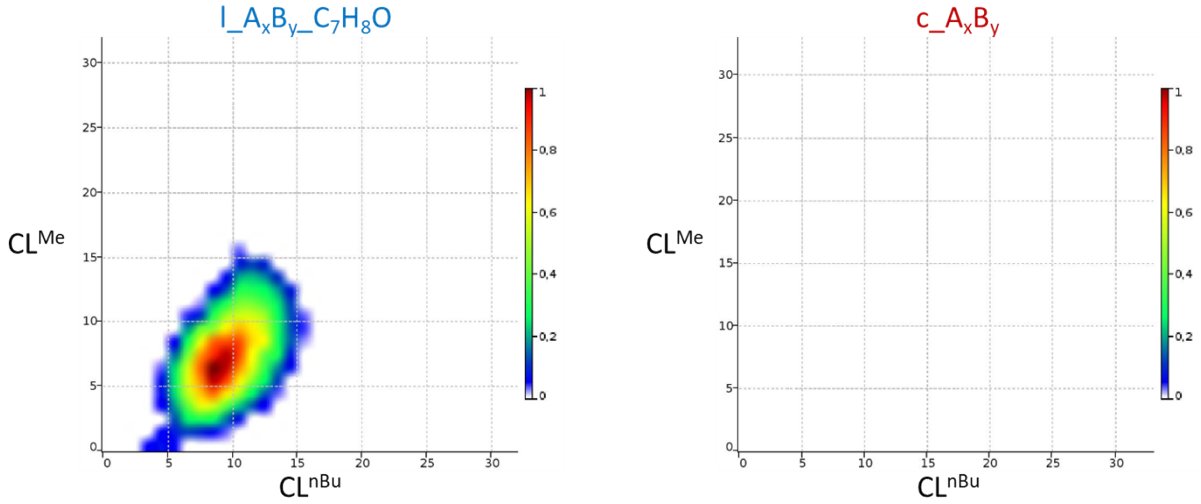

Figure S23. Contour-plots generated by the COCONUT[i] software from MALDI-ToF MS data of a P(CL$^{n\text{Bu}}$)$_x$-*co*-(CL$^{\text{Me}}$)$_y$ copolymer (Left: linear population; Right: cyclic population) (Table 1, entry 1).

[i] M. S. Engler, S. Crotty, M. J. Barthel, C. Pietsch, K. Knop, U. S. Schubert, S. Böcker, COCONUT-An efficient tool for estimating copolymer compositions from mass spectra. *Anal. Chem.*, **2015**, *87*, 5223-5231.

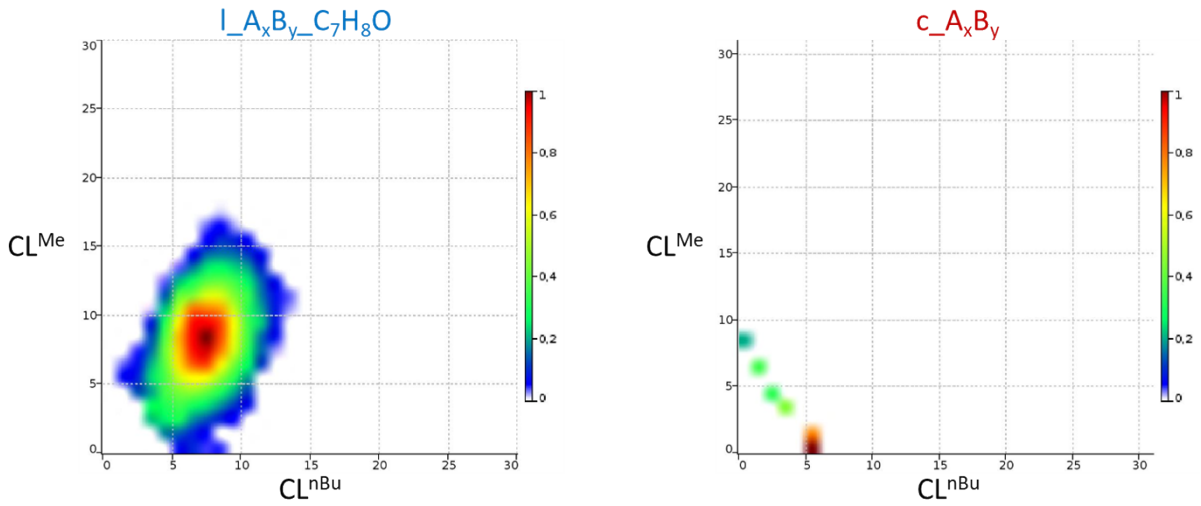

Figure S24. Contour-plots generated by the COCONUT software[i] from MALDI-ToF MS data of a P(CL$^{n\text{Bu}}$)$_x$-*co*-(CL$^{\text{Me}}$)$_y$ copolymer (Left: linear population; Right: cyclic population) (Table 1, entry 6).

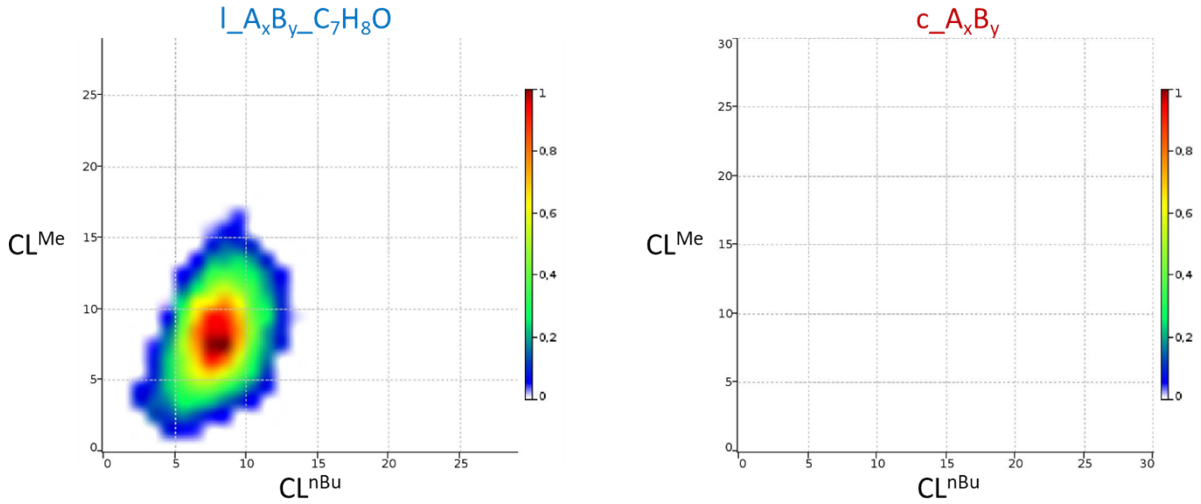

Figure S25. Contour-plots generated by the COCONUT software[i] from MALDI-ToF MS data of a P(CL$^{n\text{Bu}}$)$_x$-*co*-(CL$^{\text{Me}}$)$_y$ copolymer (Left: linear population; Right: cyclic population) (Table 1, entry 2).

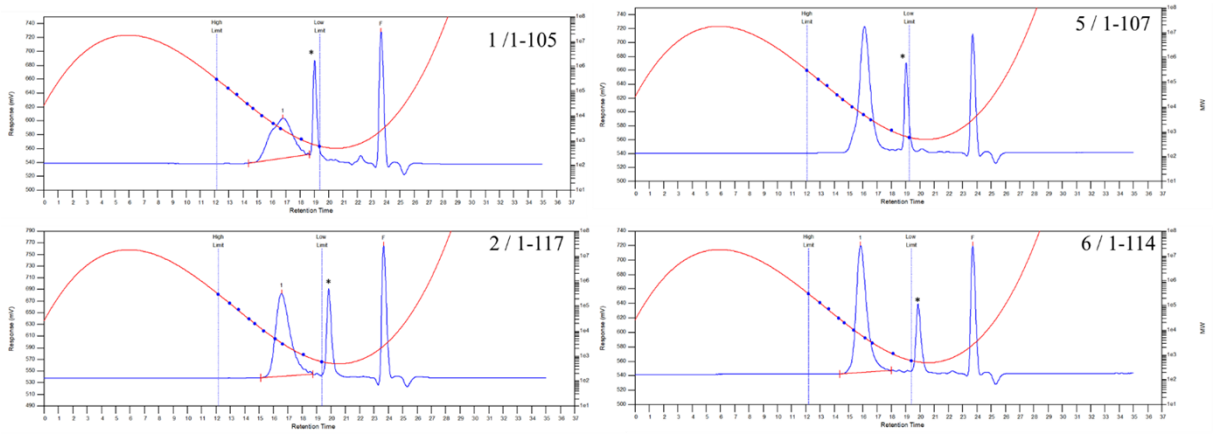

Figure S26. Representative SEC traces of homopolymers prepared from the ROP of *rac*-CL^{Me} and *rac*-CL^{nBu} with yttrium catalyst systems **1a-b**/BnOH (see Table S1, entries 1/(1-015); 2/(1-117); 5/(1-107); 6/(1-114)). * stands for signal from residual ligand catalyst.

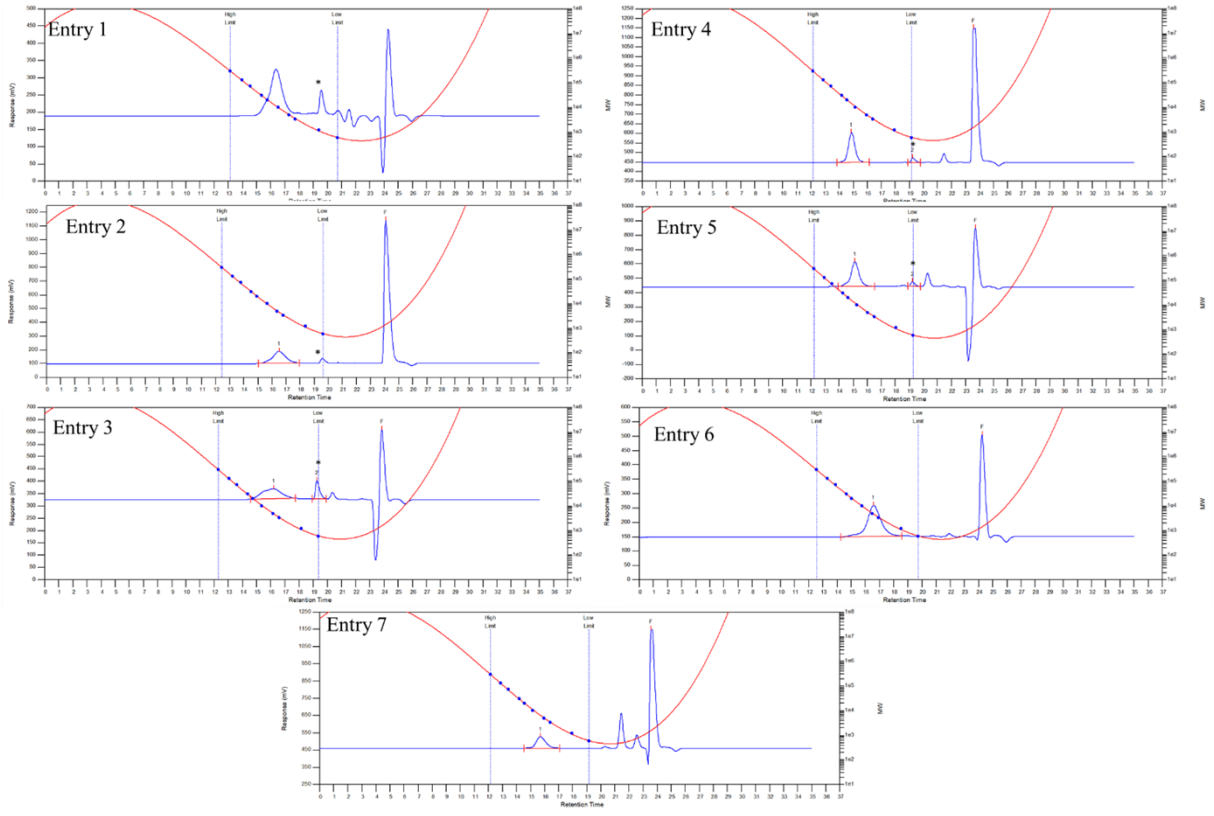

Figure S27. Representative SEC traces of copolymers prepared from the ROP of equimolar mixtures of (*S*)-CL^{Me} and (*R*)-CL^{nBu} with yttrium catalyst systems **1a-b**/BnOH (see Table 1, entries 1-7). * stands for signal from residual ligand catalyst

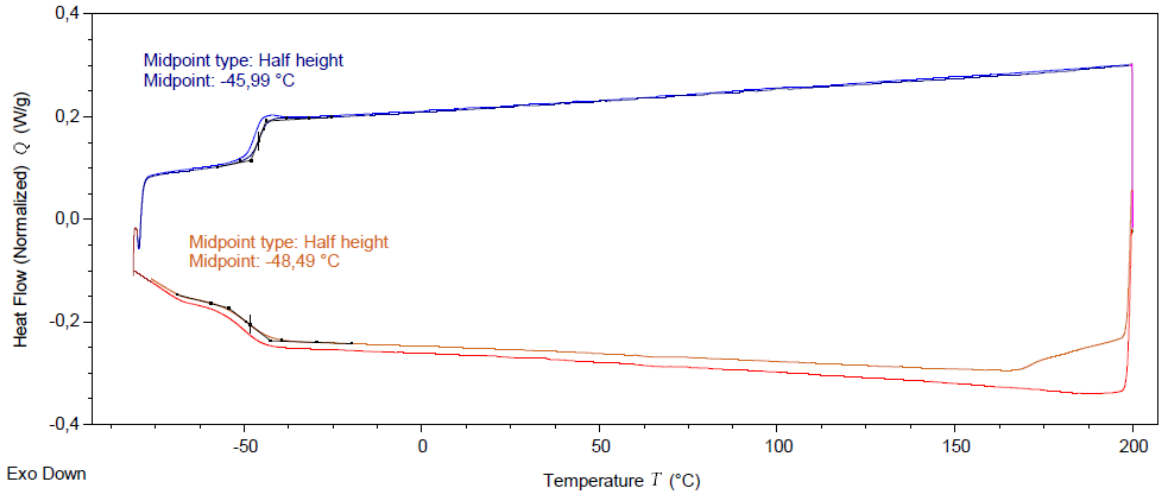

Figure S28. DSC thermogram (heating rate of 10 °C min^{-1}, second heating cycle, from −80 to +200 °C) of a PCL^{Me} homopolymer prepared from the ROP of *rac*-CL^{Me} with the **1a**/BnOH catalyst system (Table S1, entry 1 /1-105).

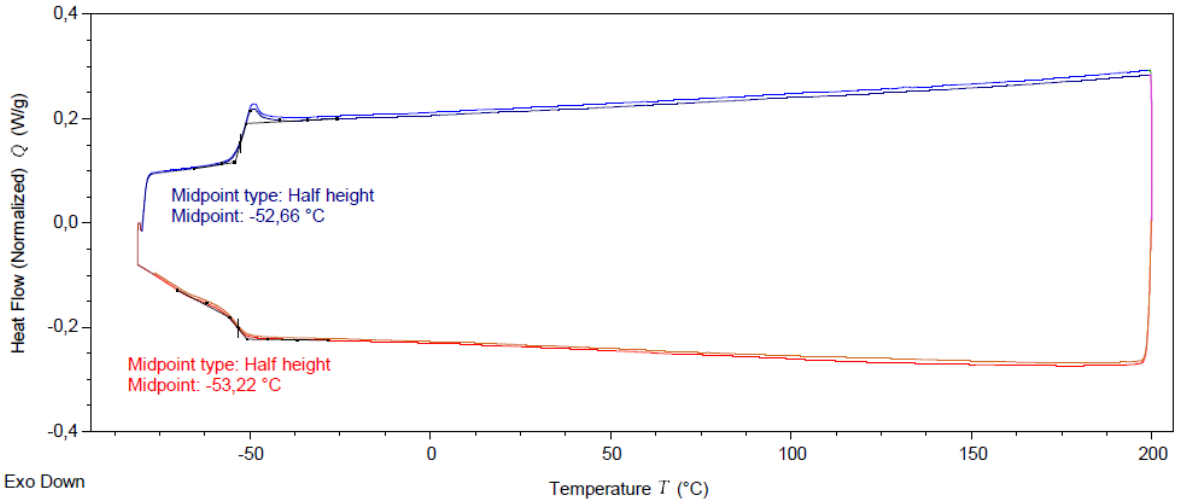

Figure S29. DSC thermogram (heating rate of 10 °C min^{-1}, second heating cycle, from −80 to +200 °C) of a PCL^{Me} homopolymer prepared from the ROP of *rac*-CL^{Me} with the Zn(BDI)/BnOH catalyst system (Table S1, entry 2 / 1-117).

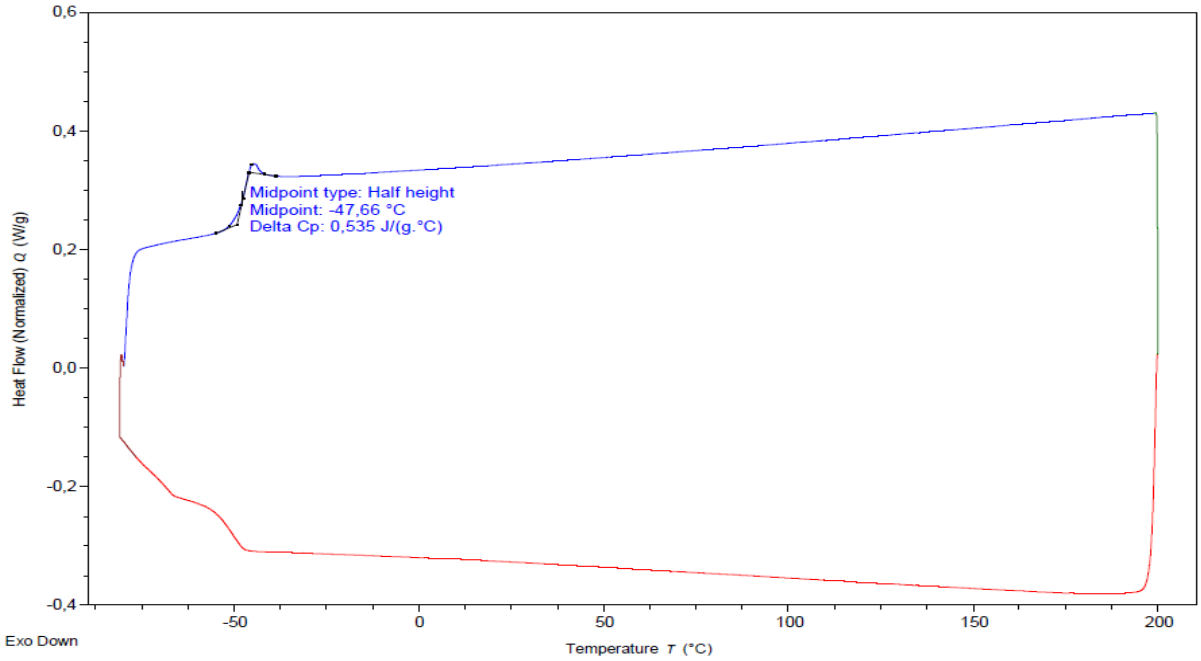

Figure S30. DSC thermogram (heating rate of 10 °C min^{-1}, second heating cycle, from −80 to +200 °C) of a PCL^{Me} homopolymer prepared from the ROP of (*S*)-CL^{Me} with the Zn(BDI)/BnOH catalyst system (Table S1, entry 4 / 1-193).

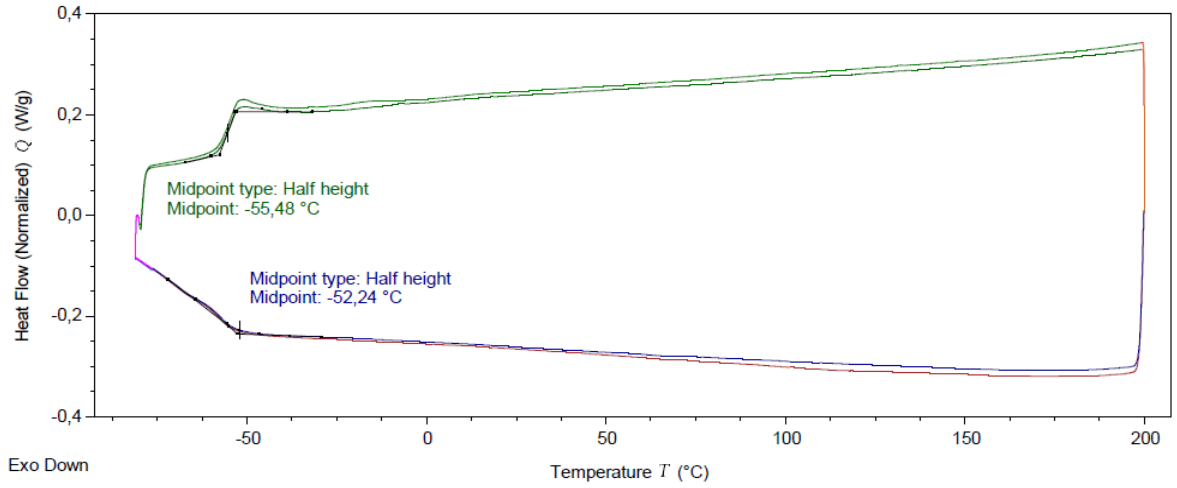

Figure S31. DSC thermogram (heating rate of 10 °C min^{-1}, second heating cycle, from −80 to +200 °C) of a PCL^{nBu} homopolymer prepared from the ROP of *rac*-CL^{nBu} with the **1a**/BnOH catalyst system (Table S1, entry 5 / 1-107).

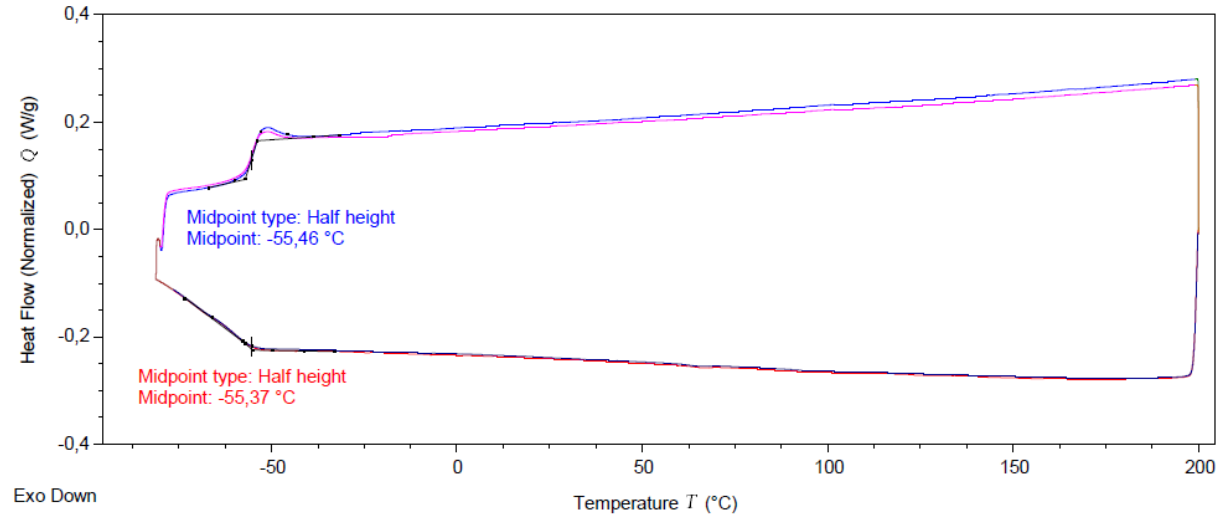

Figure S32. DSC thermogram (heating rate of 10 °C min^{-1}, second heating cycle, from −80 to +200 °C) of a PCL$^{n\text{Bu}}$ homopolymer prepared from the ROP of *rac*-CL$^{n\text{Bu}}$ with the Zn(BDI)/BnOH catalyst system (Table S1, entry 6 / 1-114).

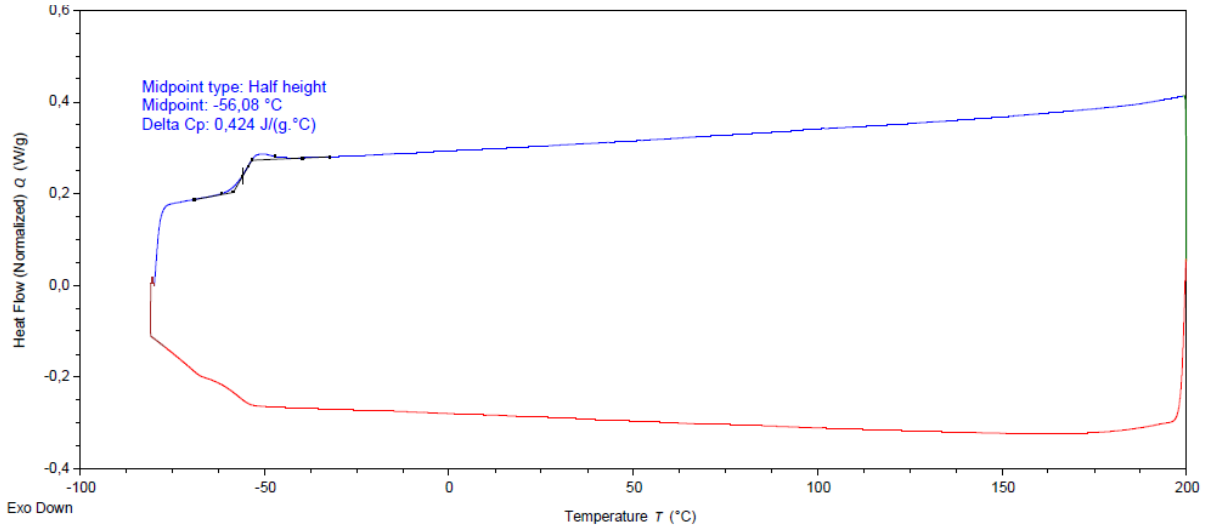

Figure S33. DSC thermogram (heating rate of 10 °C min^{-1}, second heating cycle, from −80 to +200 °C) of a PCL$^{n\text{Bu}}$ homopolymer prepared from the ROP of *rac*-CL$^{n\text{Bu}}$ with the Zn(BDI)/BnOH catalyst system (Table S1, entry 8 / 1-164).

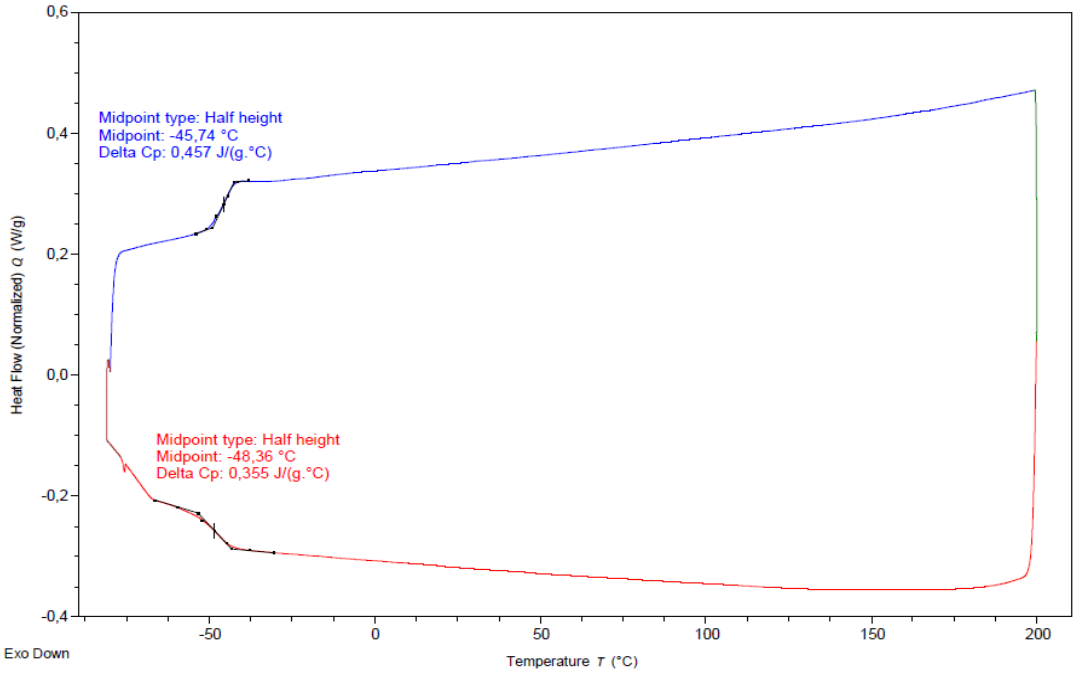

Figure S34. DSC thermogram (heating rate of 10 °C min^{-1}, second heating cycle, from −80 to +200 °C) of a P(CL^{Me}-*co*-CL$^{n Bu}$) copolymer prepared from the ROCOP of a 1:1 mixture of (*S*)-CL^{Me} and (*R*)-CL$^{n Bu}$ mediated by the **1a**/BnOH (1:1) catalyst system (Table 1, entry 1).

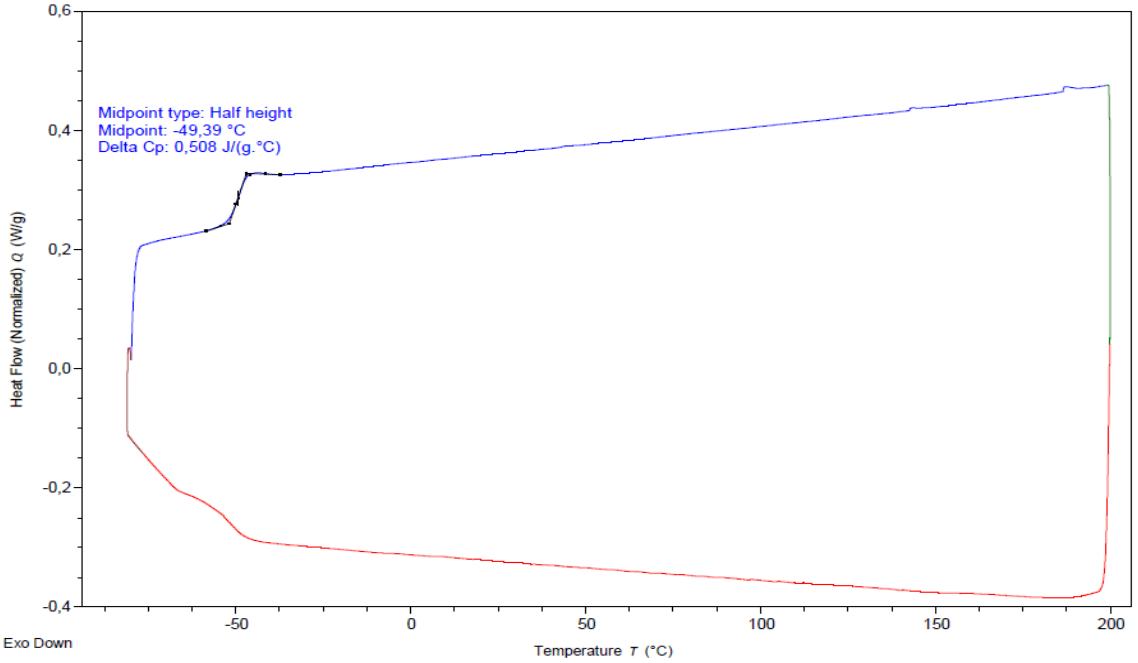

Figure S35. DSC thermogram (heating rate of 10 °C min^{-1}, second heating cycle, from −80 to +200 °C) of a P(CL^{Me}-*co*-CL$^{n Bu}$) copolymer prepared from the ROCOP of a 1:1 mixture of (*S*)-CL^{Me} and (*R*)-CL$^{n Bu}$ mediated by the **1b**/BnOH (1:1) catalyst system (Table 1, entry 6).

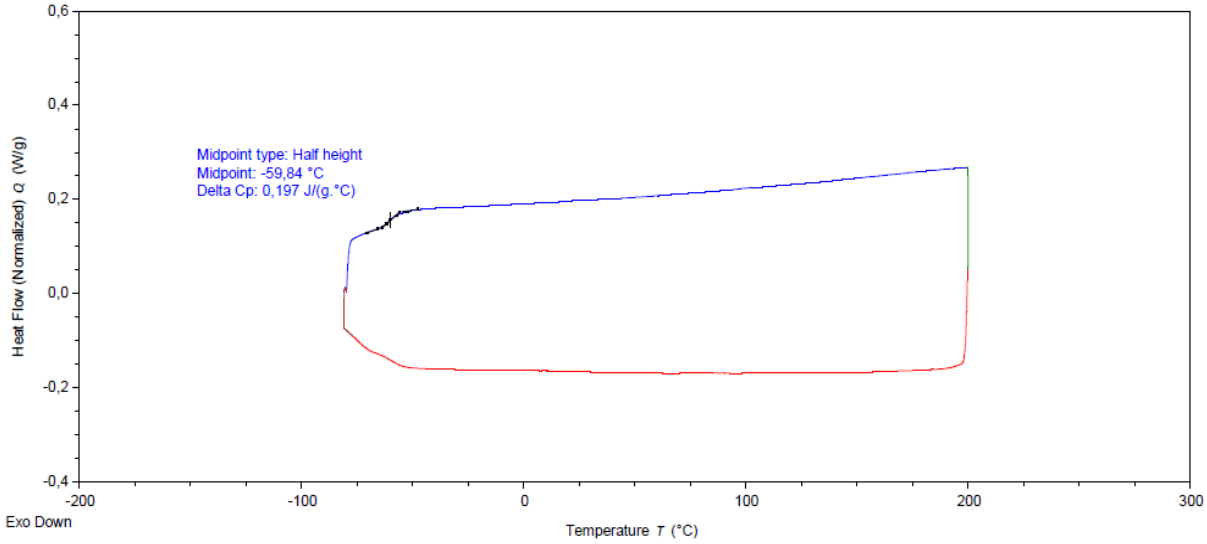

Figure S36. DSC thermogram (heating rate of 10 °C min^{-1}, second heating cycle, from −80 to +200 °C) of a P(CL^{Me}-*co*-CL^{nBu}) copolymer prepared from the ROCOP of a 1:1 mixture of (*S*)-CL^{Me} and (*R*)-CL^{nBu} mediated by the **1b**/BnOH (1:1) catalyst system (Table 1, entry 7).